TWO METHODS FOR SEPARATING HIGHER MODES OF SEISMIC SURFACE WAVES

by

Leon Horowicz

B.A. Oxford University
(1964)

SUBMITTED IN PARTIAL FULFILLMENT OF
THE REQUIREMENTS FOR THE DEGREE OF

MASTER OF SCIENCE

at the

MASSACHUSETTS INSTITUTE OF TECHNOLOGY

May, 1966

Signature of Author . . . . . .
Department of Geology and Geophysics
May 11, 1966

Certified by . . . . . .
Thesis Supervisor

Accepted by . . . . . .
Chairman, Departmental Committee
on Graduate Students

TWO METHODS FOR SEPARATING HIGHER MODES OF SEISMIC SURFACE WAVES

by

Leon Horowicz

Submitted to the Department of Geology and Geophysics on May 20, 1966, in partial fulfillment of the requirements for the degree of Master of Science at the Massachusetts Institute of Technology

This thesis is divided into two main parts concerned with two methods for isolating higher modes. The first is a technique which depends on the group velocity characteristics of the modes; it is applied to long-period Love waves generated by an earthquake and the higher modes isolated. Phase velocity dispersion curves are plotted and compared with models derived from fundamental mode studies.

In Part II a technique depending on the phase velocity dispersion characteristics is investigated, and results of a model study to isolate "Leaky" modes are shown. The possibility of extending the method to non-uniform arrays is discussed with a view to its application to earth studies.

In conclusion, the two methods are compared and their range of applicability discussed.

Thesis Supervisor: M. Nafi Toksöz
Assistant Professor of Geophysics

TABLE OF CONTENTS

FIGURES

I. INTRODUCTION

Seismic surface wave data from earthquakes have proved a useful tool in the study of the velocity distribution in the crust and upper mantle. The depth of penetration of these waves is dependent on the wavelength and, correspondingly, on the period. For crustal studies down to 50 km surface waves in the period range 50 secs and lower are most useful, while for upper mantle studies the period range 50 - 1000 secs is utilized.

The procedure to determine phase velocities is to isolate a particular mode at two locations and measure the phase change of each frequency; this is related in a known way to phase velocity. A technique often used which has the advantage that it is independent of seismometer distortion is to pick the traces up at one location as the disturbance propagates over the great circle path connecting the station and the epicenter of the event. The error in the exact location and configuration of the source can be avoided by taking pairs of events such as $G_1 - G_3$, $G_2 - G_4$,

$R_1 - R_3$, etc., in which case the distance is exactly the length of the great circle path and the phase velocity, as derived in Appendix A, is

$$C(f) = \frac{\Delta x_{12}}{\Delta t_{12} + 1/f\left(\Delta\phi_{12}(f) + N - \frac{1}{2}\right)} \qquad (1)$$

where Δx_{12} is the great circle length

Δt_{12} is the time difference between the two windows

$\phi_{12}(f)$ is the phase difference in circular units

-1/2 is introduced because of the $\pi/2$ phase shift per polar passage (Brune, Nafe and Alsop, 1961)

N is an integer which must be introduced since phases are multivalued functions.

In order to determine N the phase velocity must be known at at least one frequency to reasonable accuracy. Once this value is fixed the phase differences over all frequencies can be incremented relative to it so as to make them smoothly varying functions of frequency (Toksöz and Ben-Menahem, 1963).

Once the experimental dispersion curve is determined it can be compared with a theoretical curve for a multi-layered model and the model parameters adjusted to agree with the experimental curves (Takeuchi, Dorman and Sato, 1964). Programs to calculate such dispersion curves exist; these are based on Haskell's matrix iteration method (Haskell, 1953) with corrections for sphericity (Alterman et al., 1961) and a small correction for gravity. On the other hand, sphericity can be treated by reformulating the problem in terms of the resonant vibrations of a spherical earth (Alsop, 1963).

No mention has been made of the technique for isolating modes; most of the studies undertaken so far have been for fundamental modes with the higher modes ignored. This approximation is adequate for shallow focus earthquakes in which the higher modes are relatively unexcited. On the basis of these studies various earth models have been proposed, two of which are shown in Figure 2.

This thesis will investigate the possibility of using higher modes for earth studies; the effort will be concentrated in comparing two filtering techniques to separate higher modes from the predominant fundamental mode.

Higher modes, if properly isolated, can prove a very useful tool for studying the earth's velocity structure (Anderson and Toksöz, 1963; Kovach and Anderson, 1964). Not only do they provide a means of checking on the models derived from fundamental mode studies, but also, because of their deeper sampling ability, they should give more reliable results at depth. This fact is illustrated in Figure 1, where relative displacements with depth are shown for the first three Love modes at a period of 50 seconds for the oceanic model shown in Figure 2 (Harkrider, 1966). The displacement is relative to that at zero depth for each mode; in absolute terms the displacements for the fundamental mode are an order of magnitude greater than those for the higher modes. Higher modes are also useful for investigating

the low-velocity zone; over certain period ranges the lobes of the higher modes are effectively trapped in the low-velocity zone and this is responsible for channel waves often observed.

Group and phase velocity dispersion curves for fundamental and higher Love modes for an oceanic and shield model (Toksöz and Anderson, 1965; Harkrider, 1966) are shown in Figure 3. On the basis of arrival alone (group velocity) mode separation is not possible, particularly in the period range up to 70 seconds, without some special filtering technique.

In Part II of this thesis a filtering technique developed by Pilant (1963) is used to effect mode separation. The principle is that a varying band pass filter is applied to the seismic trace in such a way that the pass band is modeled around the dispersion curve of the particular mode of interest. The technique has already been applied by Toksöz and Anderson (1966) to separate interfering phases of fundamental modes.

This method is not suitable in the frequency range in which the group velocity curves for different modes cross, and in Part III another filtering technique is investigated which depends on the phase velocity characteristics of the modes; these, as shown in Figures 6 and 7, are more separated. In this case the principle is that signals from an array are processed by convolving each with an appropriate two-point operator and summing; the net effect is to pass a certain band of phase velocities.

II. GROUP VELOCITY FILTERING FOR MODE SEPARATION

In this chapter a mode separation technique developed by Pilant (1963) is used to isolate higher modes from long-period (40 - 400 secs) surface wave Love data. The technique is incorporated in a computer program and used on digital data. Different frequency pass bands are applied between specified group velocity (time) arrivals in such a way that the pass band is modeled around the particular mode to be isolated. Figure 3 shows theoretical group velocity curves of an oceanic and shield model (Toksöz and Anderson, 1965; Harkrider, 1966) for fundamental and higher Love modes; around these are modeled suitable time-varying frequency pass bands which will effect mode separation. Appendix B discusses some of the more pertinent details of the "Sliding" Filter program. For higher mode studies the input traces must be truncated before the arrival of the fundamental mode in the frequency range at which it would be passed by the filtering process. This technique

is applied to data from an event recorded in 1960 and suspected of being relatively rich in higher harmonics, and its ability to isolate these higher modes is investigated.

An event was recorded by long-period instruments at Pasadena on June 12, 1960; the C.G.S. gave its location and origin time as 36°S, 98°W; 7^h 19' 43" G.M.T. The great circle path appropriate to the event is shown in Figure 4, and it is suspected of having dispersion characteristics somewhere between those of the oceanic and shield model shown in Figure 2 (Toksöz and Anderson, 1965).

A total of three phases are digitized; the specifications for these are given in Table I and the traces are shown in Figure 5a. These horizontal, E-W records contain, as well as Love waves, residual Rayleigh disturbances which are the projections of the longitudinal Rayleigh motion in the E-W direction. For the purposes of this analysis the Rayleigh components in all the E-W records were assumed to be small. This is justified as the great circle path for the event passes through Pasadenaclose to the N-S direction (azimuth

163°), so that the component of longitudinal Rayleigh motion in the E-W direction is small.

Figure 3 shows the varying band pass filters applied to appropriate records to separate the fundamental, first and second higher Love surface wave modes. In applying the filtering program described in Appendix B it is seen that sufficient frequency rejection is obtained with filters of length 360 secs (120 points for data digitized at three-second intervals). With filters of this length the criterion for over 75% rejection discussed in Appendix B is satisfied for frequencies 0.0015 c.p.s. outside the specified pass band, and it is observed from Figure 3 that on the basis of this criterion the higher modes are sufficiently separated. The corresponding traces filtered to isolate the fundamental, first and second higher Love modes are shown in Figures 5b and 5c.

Phase velocities can be found without including the error in source location only for the pair $G_1 - G_3$; this

error is expected from travel time calculation to be fairly substantial and of the order of 1° to 3° (100 - 300 km). Thus, if all the records are to be utilized, it is first necessary to correct for it. This is done by computing phase velocity dispersion curves for the fundamental Love mode determined by using the pairs of events $G_1 - G_3$, $G_1 - G_2$, $G_2 - G_3$ and equation (A.3) derived in Appendix A, with the appropriate factor 1/2 or 1/4, depending on the pair of phases used.

For the pair $G_1 - G_3$ Δx is the great circle path which is known to high accuracy (40015 km). The corresponding values of Δx from the pairs $G_1 - G_2$, $G_2 - G_3$ are adjusted so that they agree with the dispersion curves found from the pair $G_1 - G_3$ over a reasonably large range of periods. On this basis it is possible to assign an epicentral correction, but such a method of correcting for the epicentre has a number of errors. Firstly, it assumes that the source radiates symmetrically. Secondly, the pairs of events $G_1 - G_3$, $G_2 - G_3$, $G_1 - G_2$ sample the

earth in different ways, so that the dispersion curves should be slightly different. Nevertheless, this method of correction is adopted since it is the simplest. The assumption of source symmetry does not justify a more detailed approach in which paths are analysed in terms of oceanic and continental components to determine dispersion curves. An epicentral correction of 180 km away from Pasadena is used and the results of dispersion calculations from the three sets of traces shown in Table IIa; the dispersion curves are drawn in Figure 6 and compared with those for the oceanic and shield model. Agreement is good in the period range 100 - 300 seconds; below 100 seconds no agreement is expected or found, since it is the region where the higher modes are included together with the fundamental (see Figure 3). Using the corrected epicentral distances the group velocity arrivals at which the band pass filters jump are determined to a greater accuracy, although this is not so critical, since the group velocity curves are steep in this region. In isolating higher modes the input traces

are truncated at appropriate group velocity arrivals so that the fundamental mode is not included. This is done partly by observing the traces and partly from what is expected on the basis of theoretical group velocity curves (Figure 3). Observation often shows the onset of another mode by the peculiar inflection of the trace; this is observed for G_1 at $07^h\ 50'\ 40''$ (see Figure 5a). The results of filtering using the parameters shown in Figure 3 are the fundamental and higher mode traces drawn in Figures 5. With the assumption that the part of the mode within each time gate is transient, no limitation is placed on frequency sampling (see Appendix D). Fourier transforms of the traces are derived by a Fourier analysis program using the trapezoid rule (Alexander, 1963).

With test values for phase velocities from the theoretical dispersion curves for each of the modes, the appropriate value of N in equation (A.3) is determined. The phases (f) and (f) are incremented to make them smoothly varying functions of frequency. The above procedure is all incor-

porated in a program written to determine phase velocities over the whole range of periods using equation (A.3) with the factor 1/2 for the set $G_1 - G_3$ and 1/4 for the sets $G_1 - G_2$, $G_2 - G_3$. A check must be made before the results are accepted that the phases $\phi_1(f)$ and $\phi_2(f)$ are not incremented in regions of instabilities and that the modes have appreciable amplitudes at the frequencies accepted. The results of the higher mode phase velocity determinations are shown in Table II and plotted in Figure 7, where they are compared with the dispersion curves appropriate to the oceanic and shield model (Harkrider, 1966).

The fundamental Love mode study indicates that an earth model of approximately the shield type is appropriate and this is borne out by the higher mode dispersion curves at periods below 140 and 70 seconds for the first and second higher modes respectively. However, at longer periods both dispersion curves diverge appreciably from this model.

The distributions derived from fundamental mode studies are not too reliable at great depths because the sampling

characteristic of the fundamental mode gives much more weight to shallow depths. The results of the higher mode study seem to indicate that at large depths the shear velocities of the oceanic and shield model are too small by a few tenths of a km/sec. Higher modes have maxima in displacement at depths of approximately 500 - 700 km in the period range of 160 and 90 seconds for the first and second modes respectively (Harkrider, 1966) and this is the region in which a correction has to be made.

The scatter of results for different pairs is expected because the paths are different, but is also in part due to the asymmetric value of the source and the method of estimating the epicentral correction. These facts lead one to place the most reliance on the $G_1 - G_3$ measurements which are accurate. There is some doubt about the validity of the second higher mode results, as no account has been taken of the third higher mode, which is assumed to be unexcited. Provided that the modes are sufficiently uncontaminated the only appreciable error in phase velocity as determined

from equation (A.3) for the set G_1 - G_3 is the phase difference $\Delta\phi_{12}(f)$. This depends on the method of computing the Fourier transform and the assumption of pulse transience within the time gate used. However, the major term in the denominator of equation (A.3) is ΔT_{12} = 8760. Provided that the integer value N is correct, the error in $\Delta\phi_{12}(f)$ is unlikely to be more than 0.1; this at a period of 100 seconds would give an error of 1/10% in the phase velocity and make the results accurate to at least the second decimal place.

III. MODE SEPARATION BY PHASE VELOCITY FILTERING

The need to go into some other technique of filtering in the range where the group velocity curves intersect was indicated in the introduction. In this section the technique of phase velocity filtering is investigated, first for a uniformly spaced array for which the results of a model study indicate that this technique is quite effective in separating "leaky modes" from the more predominant Rayleigh modes. The possibility of extending it to non-uniform arrays is discussed; this is the part which is of particular interest to real earth studies since at present a uniform array of large enough aperture for mantle studies does not exist. The problem of non-uniformity of response of each of the elements in the array is an obstacle in this type of filtering system and its effect must be considered.

Phase Velocity Filtering with Uniformly Spaced Array

Phase velocity filtering is effected by convolving each one of a set of digitized traces from a uniform linear

array with an appropriate two-point operator in the time domain which determines the particular range of phase velocities passed. The theoretical justification and the restrictions of the technique are derived in Appendix C. This procedure is applied to a model study to isolate "leaky" modes from the Rayleigh modes.

The model used is shown in Figure 8; one of its features irrelevant to the present study is that the brass-steel interface is sloping; however, the tilt over the range of values for which data are taken is small enough that it is a good approximation to assign an average thickness (Kuo, 1963).

Disturbances in the model are excited by a piezo-electric source crystal attached to the top of the brass layer; these acoustical vibrations are picked up by another crystal touching the side of the model and are fed into a digitizer.

The disturbances propagating through the model can be analysed in terms of modes; theoretical dispersion curves

for a model with a 4-cm brass layer are shown in Figure 9. It is necessary to attenuate the Rayleigh modes and for this phase velocity filtering is applied between 3.3 mm/μsec and 10 mm/μsec. With space sampling at 10 mm and time sampling at 1 μsec, this would be equivalent to setting the parameters $C_1 = 1/3$, $C_2 = 1$ in equation (C.6). The appropriate convolution operators are shown in Figure 10 and the corresponding double Fourier transform in Figure 11.

A series of 24 traces at 10 mm separations are digitized, at a depth of 40 mm, in order that the fundamental Rayleigh mode, which at the surface would be an order of magnitude greater than the other modes, would be comparable to them. The convolution process is applied to the first and last twelve traces to generate two filtered traces separated by 120 mm. One such set of filtered and unfiltered traces is shown in Figure 12. The enhancement of the earlier portion of the trace with the "leaky" modes compared to the later part is observed. The disturbance

after the fundamental Rayleigh mode consists mainly of flexural waves which are of no interest to this investigation.

The method used to determine phase velocities is described in Appendix A. The number of correlation lags taken to compute the transfer function depends on the noise content of the trace; in general, any trace can be divided into signal and noise

$$p_1(t_N) = S_1(t_N) + n_1(t_N) \tag{2}$$

Noise consists of a random component uncorrelated to the signal and a component which is in some way correlated to the signal; in the case of the model study, reflections from the sides and bottom of the model are examples of the latter.

The correlations are

$$\varphi_{11}(t_N) = \sum_{N'} [S_1(t_{N'}) + n_1(t_{N'})][S_1(t_{N'-N}) + n_1(t_{N'-N})] \tag{3}$$

$$= \varphi_{S_1S_1}(t_N) + \varphi_{n_1n_1}(t_N) + \varphi_{S_1n_1}(t_N) + \varphi_{n_1S_1}(t_N)$$

and similarly

$$\varphi_{12}(t_N) = \varphi_{s_1 s_2}(t_N) + \varphi_{n_1 n_2}(t_N) + \varphi_{s_1 n_2}(t_N) + \varphi_{n_1 s_2}(t_N) \qquad (4)$$

In both cases it is the first terms only that are of interest and over a certain range of correlation lags these predominate. Noise uncorrelated to the signal contributes only through the term $\varphi_{n_1 n_1}(t_N)$. In this model study this consists of digitization noise and electrical pickup, and should be small compared with other terms. Coherent noise contributes through the terms $\varphi_{s_i n_j}(t_N)$ and is largest at greater lags.

A time gate from the first P break to the Rayleigh break is used for each of the filtered traces. In this region are included the "leaky" modes and part of the higher Rayleigh modes which begin at the first shear break; the latter have been attenuated by phase velocity filtering. The two filtered traces are fed into a package program to calculate phase velocities by the method described in

Appendix A. On the assumption that the distinct disturbances between 50 - 100 μsecs and 100 - 150 μsecs observed on the filtered trace in Figure 12 represent different modes, fifty lags are taken in the correlations to compute the transfer function. These would include most of the information from these "hypothesized" distinct modes and, hopefully, minimize the coherent noise while including most of the information from the modes.

The experimental phase velocities derived are shown in Figure 13 and compared with those computed theoretically. Various possibilities exist for phase velocities, since the phases are multivalued functions, and by a more detailed study of the excitation functions for the various modes it is possible to interpret the range of frequencies in which each curve is valid. A detailed investigation of the results of the model study is left to the end of this section.

Phase Velocity Filtering with a Non-Uniform Array

The fact that uniform arrays of large enough apertures do not exist necessitates an investigation of the applicability of this technique to non-uniform arrays.

Phase velocity filtering should prove useful in the period range below 50 sec, where group velocity curves for surface wave modes intersect, requiring arrays of dimensions of the order of 400 - 500 km. At present the only array that comes near to meeting these requirements is LASA, which is shown in Figure 14a; the array consists of 21 sub-arrays covering an area of radius 100 km, each containing 25 seismometers spread over a circular region of radius 3 - 5 km. A possible linear array that can be constructed from LASA which is symmetrical about its center is shown in Figure 14b. One seismometer from each of the sub-arrays numbered is projected in a NE direction; the particular seismometer is chosen so that the separation between them is close to 10 km. The linear array formed in this way is equivalent to a 10-point uniform array with two locations symmetrical about the center missing. The appropriate space domain sampling operator is

$$\sum_{\substack{m=-(M+\frac{1}{2}) \\ \vdots \\ 0}}^{\substack{0 \\ \vdots \\ +(M+\frac{1}{2})}} \left\{ \delta(x - m\Delta x) - \delta(x + m\Delta x) \right\} - \delta\left(x + \tfrac{9}{2}\Delta x\right) \qquad (5)$$

where M is 5 and δ represents the delta function. The complex Fourier transform of this function is shown in Figure 15 and is

$$\frac{SIN(10\pi\bar{k})}{SIN(\pi\bar{k})} - COS(7\pi\bar{k}) \qquad (6)$$

where the first term represents a finite symmetrical uniform linear array of 10 points and the second term the effect of two missing locations. The frequency-wave number characteristics of this system are obtained by convolving the characteristics of the exact phase velocity filter with equation (6) over dimensionless wave number. Phase velocity filtering should be effective in the wavelength range 10 - 50 km; 10 km is the lower limit set by aliasing and 50 km the upper limit due to the finiteness of the array; this would correspond to periods in the range 2 - 10 sec for surface waves.

In order that two-point time domain filtering be applied the following conditions are imposed on the parameters C_1 and C_2 in equation (C.6) (Appendix C):

$$C_2 = 1/N \; ; \; C_1 = 1/(N+2), \text{ or } 1/(N+6), \text{ or } 1/(N+10) \text{ etc.}$$

where N is an odd integer.

As an example, consider the case $x = 10$ km, $t = .15$ sec, $N = 15$. The cutoff phase velocities for the filtering process are, taking $C_2 = 1/N$, $C_1 = 1/(N+2)$:

lower cutoff $\left(\frac{1}{N+2}\frac{\Delta x}{\Delta t}\right) = 3.921$ km/sec

upper cutoff $\left(\frac{1}{N}\frac{\Delta x}{\Delta t}\right) = 4.444$ km/sec

For an event not in the NE direction it is necessary to take projections of the linear array in the direction of the event, resulting in smaller overall dimensions. On the other hand, many other suitable linear array systems can be constructed from LASA and it is necessary to investigate the possibilities open for each event.

In a region containing a high density of stations, for example the United States, it is always possible to construct

a linear array for which the stations are separated by some integral multiple of a finite distance Δx and the missing locations (if they are symmetrically placed) can be treated as in the LASA example. In general, the appropriate space sampling operator is

$$\sum_{m=-(M+\frac{1}{2})}^{m=+(M+\frac{1}{2})} \left\{\delta(x-m\Delta x)+\delta(x+m\Delta x)\right\} - \sum_{n=N_i+\frac{1}{2}} \left\{\delta(x-n\Delta x)+\delta(x+n\Delta x)\right\} \quad (7)$$

which has a Fourier transform of

$$\frac{\sin\left[2\pi\bar{k}(M+1)\right]}{\sin(\pi\bar{k})} - \sum_{n=N_i+\frac{1}{2}} \cos\left[\pi\bar{k}(2n+1)\right] \quad (8)$$

The larger the number of missing locations N_i, the less effective the process becomes for phase velocity filtering.

The requirement for the system to be symmetrical about some origin is so that no imaginary terms occur in the complex Fourier transform of equation (7), which in real terms is equivalent to requiring both cosine and sine transforms. This would tend to make the system ineffective for simple phase velocity filtering, so that a symmetrical system seems necessary.

In the period range up to 10 sec phase velocities are relatively well separated (Anderson and Toksöz, 1963; Kovach and Anderson, 1964) and phase velocity filtering using the array discussed above, together with frequency filtering, should be effective in isolating some portions of the higher modes; whereas on the basis of group velocity it would not be possible in this period range. The possibility of isolating higher modes from the fundamental mode when the record contains both seems more remote, since the amplitude of the fundamental mode may be an order of magnitude greater than the higher modes, and this would require rejection capabilities for the filter of -40 dbp (99% amplitude) in the region of the fundamental mode. It seems, therefore, that the technique would be more useful to separate interfering higher modes from each other.

Discussion of Results of Model Study

The results of the model study indicate good agreement for the PL23 mode in the frequency range 90 - 140 kc; for the PL24 mode the results are poor while for the PL22 mode they are bad.

The source spectrum, Figure 16, shows that excitation is predominantly in the frequency range 50 - 250 kc, which may be why the results are poor for the PL22 mode. A limited number of lags are used in computing the transfer function so it is necessary to look for agreement in the region in which group velocity curves (Figure 17) have maxima and minima and are relatively undispersed, that is, between 2 mm/μsec and 4 mm/μsec. Also, with the time gate cut at the first Rayleigh break (1.97 mm/μsec), parts of the group velocity minima for the "leaky" modes are cut out.

Previous studies (Laster et al., 1962) have shown that there is substantial correlation between excitation minima, attenuation minima and group velocity maxima; the latter two points are shown in Figures 17 and 18. For "leaky" modes at sufficient distance from the source it is attenuation that determines the amplitudes of the modes. On the basis of this alone it would seem that in the region 120 kc - 140 kc the PL24 mode would predominate over the PL23 mode; however, the method of computation does not "see"

the well-dispersed PL24 mode in this frequency range. The anomalous nature of the group velocity for the PL24 mode above 140 kc explains why agreement for this mode is not so good, as well as the fact that no account has been taken of higher PL modes.

IV. APPLICATION OF THE TWO TECHNIQUES FOR EARTH STUDIES

On the basis of the results of the two studies undertaken and described in Parts II and III of this thesis, the two methods of mode separation are shown to be quite effective. The group velocity technique is much easier to implement, requiring only one station, and hence is free from errors associated with the reproducibility of seismometers. The method will prove to be useful for higher Love and Rayleigh modes above 40 - 50 seconds period for which the group velocity dispersion curves are sufficiently well separated (Anderson and Toksöz, 1963; Kovach and Anderson, 1964). If dispersion curves are required at lower periods, phase velocity filtering will prove useful, particularly for the first few higher modes. However, fundamental mode studies give a fairly accurate picture of the velocity distribution in the upper mantle down to 300 - 400 km, so that in higher mode studies interest will be focused on longer periods which sample the earth at greater depths. Group velocity filtering

techniques are sufficiently adequate at long periods and it seems unlikely that the more difficult phase velocity filtering will be used for such studies, particularly considering the large dimensions required for arrays. This latter technique is more useful for crustal studies over regional paths and may be extended if sufficiently large arrays are found to study the low velocity zone.

Part III has already indicated the possibility of errors in the models derived from fundamental mode studies at depths of 500 - 700 km, and more work needs to be done in this area.

Acknowledgement

I would like to thank Dr. M. Nafi Toksöz for his valuable advice and assistance in helping me carry out the research which constituted Part II of the thesis. This work was supported by the Air Force Office of Scientific Research under Contract AF-49(638)-1632.

The model study included in Part III was done during the summer of 1965 while I was working for Texas Instruments. I would like to thank Texas Instruments for allowing me to include this work in my thesis; and, in particular, Stan Laster, Frank Linville and Bob Warren for their help and encouragement.

References

Alexander, S.S., "Crustal structure in western United States from multi-mode surface wave dispersion", Ph.D. thesis, California Institute of Technology, 1963.

Alsop, L.E., "Free spheroidal vibrations of the earth at very long periods", Bull. Seism. Soc. Am. 53, 483, 1963.

Alterman, Z., H. Jaroch and C.L. Pekins, "Propagation of Rayleigh waves in the earth", Geophys. J. 4, 219, 1961.

Anderson, D.L., and M.N. Toksöz, "Surface waves on a spherical earth: 1. Upper mantle structure from Love waves", J. Geophys. Res. 68, 3483, 1963.

Brune, J., J.E. Nafe and L.E. Alsop, "Polar phase shift of surface waves on a sphere", Bull. Seism. Soc. Am. 51, 247, 1961.

Embree, P., J.B. Burg, and M.M. Backus, "Wide-band filtering - the 'pie slice' process", S.E.G. Yearbook, 186, 1963.

Foster, M.R., R.L. Sengbush and R.J. Watson, "Design of suboptimum filter systems for multi-trace seismic data processing", Geophys. Prosp. 12, 173, 1964.

Harkrider, D.G., "Surface waves in multilayered elastic media. 2: Higher mode spectra and spectral ratios from point forces in plain layered earth model", Bull. Seism. Soc. Am., to be published, 1966.

Haskell, N.A., "Dispersion of surface waves on multilayered media", Bull. Seism. Soc. Am. 43, 17, 1953.

Kovach, R.L., and D.L. Anderson, "Higher mode surface waves and their bearing on the structure of the earth's mantle", Bull. Seism. Soc. Am. 54, 161, 1964.

Kuo, J.T., "Model studies of sloping interface on Rayleigh waves", J. Geophys. Res. 68, 6187, 1963.

Laster, S.J., A.F. Linville and J.G. Forman, "Basic research in crustal studies", Semi-Annual Technical Reports Nos. 1, 2 and 3, Texas Instruments, 1965.

Lee, Y.W., Statistical Theory of Communication, John Wiley & Sons, Inc., 1960.

Pilant, W.L., personal communication, 1963.

Toksöz, M.N., and A. Ben-Menahem, "Velocity of mantle Love and Rayleigh waves over multiple paths", Bull. Seism. Soc. Am. 53, 741, 1963.

Toksöz, M.N., and D.L. Anderson, "Velocity of long-period surface waves and structure of the upper mantle", Am. Geophys. Un. Transactions, 1965.

Toksöz, M.N., and D.L. Anderson, "Phase velocities of long-period surface waves and structure of the upper mantle", J. Geophys. Res. 71, 1649, 1966.

APPENDIX A

Method of Computation of Phase Velocities

Consider two disturbances $p_1(t)$, $p_2(t)$ at locations x_1, x_2; each has a complex Fourier transform $P_1(f)$, $P_2(f)$ such that

$$p_1(t) = \int_{-\infty}^{+\infty} P_1(f)\, e^{2\pi i f t}\, df$$
$$p_2(t') = \int_{-\infty}^{+\infty} P_2(f)\, e^{2\pi i f t}\, df \qquad \text{(A.1)}$$

where

$$\text{ARG.}[P_1(f)] = 2\pi N_1 - \phi_1 = 2\pi f (x_1/C(f) - t_1)$$
$$\text{ARG.}[P_2(f)] = 2\pi N_2 - \phi_2 = 2\pi f (x_2/C(f) - t_2') \qquad \text{(A.2)}$$

The terms t_1, t_2' are necessary to relate the two time scales t, t' so that $t_o' - t_o = t_2' - t_1$. $C(f)$ is the phase velocity at a frequency f and N_1, N_2 are integers, necessary since

phases are multivalued functions. Subtracting equations (A.2) gives

$$C(f) = \frac{X_2 - X_1}{t'_2 - t_1 + 1/f\left[\frac{(\phi_1 - \phi_2}{2\pi} + N\right]} \qquad \text{(A.3)}$$

In part I the method used to compute phase velocities is to directly take the Fourier transform of two traces, determine an appropriate value for the integer N from a previous knowledge of several dispersion points, and use equation (A.3). A 1/4 term is added for each extra polar passage one of the paths describes over the other (Brune, Nafe and Alsop, 1961). This is an adequate procedure when noise can be ignored, which is not considered to be the case in the model study for which a different technique is used.

In the model study the phase change appropriate to each frequency is determined from the time domain transfer function $T(t_N)$ which, when convolved with $p_1(t)$ gives $\overline{p_2}(t)$; this transfer function is determined on the basis of a mean square error criterion. The convolution process gives:

$$\overline{P_2}(t_N) = \sum_{N'} T(t_{N'})\, P_1(t_{N-N'}) \qquad \text{(A.4)}$$

Taking Fourier transforms of both sides of equation (A.4):

$$\overline{P_2}(f) = H(f)\ P_1(f)$$
$$\text{ARG}[H(f)] = \text{ARG}.[\overline{P_2}(f)/P_1(f)] = \overline{\phi_2} - \phi_1 \qquad \text{(A.5)}$$

where H(f) is the Fourier transform of $T(t_{N'})$. ARG H(f) is close to $\phi_2 - \phi_1$ if $\bar{P}_2(f)$ is close to $P_2(f)$. The mean square error criterion ensures this since it requires that

$$\frac{\partial}{\partial T(t_{N'})}\left[P_2(t_N) - \overline{P_2}(t_N)\right]^2 = 0 \qquad \text{(A.6)}$$

Applying the results obtained from Lee (1960) to the digital case gives

$$\sum_{N'}\left[T(t_{N'})\,\varphi_{11}(t_{N-N'})\right] - \varphi_{12}(t_N) = 0 \qquad \text{(A.7)}$$

where

$$\varphi_{11}(t_N) = \sum_{N'} p_1(t_{N'})\, p_1(t_{N'-N})$$
$$\varphi_{12}(t_N) = \sum_{N'} p_2(t_{N'})\, p_1(t_{N'-N}) \qquad \text{(A.8)}$$

Equation (A.7) is valid for all values of t_N since, unlike the case dealt with by Lee, the filter $T(t_N)$ is realizable for all values of t_N. If a total of N lags are computed for the correlation then at the most N filter coefficients can be formed from the N equations (A.7).

APPENDIX B

"Sliding" Filter Program by Pilant

This program was written by W.L. Pilant (1963) and part of it modified by M.N. Toksöz. The program takes consecutive portions of a digital record and filters each with a specified frequency pass band. Starting with an initial low cut EPS1 and high cut EPS2 these are incremented at each jump by amounts DEL1 and DEL2 which are constant; the former is limited to positive values. This filtering is carried out in the time domain by convolving each portion of the digital trace with an appropriate time domain filter. For a pass band between f_1 and f_2 this is

$$x(t) = \tau \int_{-f_2}^{+f_2} e^{2\pi i f t}\, df - \tau \int_{-f_1}^{+f_1} e^{2\pi i f t}\, df$$

$$= \tau \left[\frac{\sin(2\pi f_2 t)}{\pi t} - \frac{\sin(2\pi f_1 t)}{\pi t} \right]$$

$$= \frac{\tau \cos(2\pi f_2 t) \sin[2\pi (f_2 - f_1) t]}{\pi t} \qquad \text{(B.1)}$$

τ is a time factor to make the right-hand side dimensionless. The function given by equation (B.1) is sampled by a digital smoothing operator

$$\delta(t - I\Delta t)\,\frac{SIN(\pi t/N\Delta t)}{\pi t/N\Delta t} \qquad \text{(B.2)}$$

where I is an integer that has values between $-N$ and N. This smoothing operator is more useful than simple truncation which introduces a substantial amount of higher harmonics. The actual frequency characteristics of the finite smoothed time domain operator are obtained by convolving the Fourier transforms of equations (B.1) and (B.2). The Fourier transforms of equation (B.2) for various lengths of the filter operator are shown in Figure 19. The convolution process has the effect of extending the range of the frequency pass band; the one-quarter width of the main lobe of each of these smoothing operators shown by arrows in Figure 19 will determine the frequency beyond the specified pass band at which rejection is over 75% of that at the center; this is chosen as the criterion for good rejection.

The two bases for deciding on the length of the filter operator used which is a constant for the program are:

1) sufficient frequency rejection is obtained for other modes;

2) the length of the filter operator is not so large that the convolution process introduces other modes.

Looking at the group velocity curves for Love modes (Figure 3), it is seen that the second criterion is satisfied for all phases because of the steepness of the dispersion curves in the range of frequencies of interest, provided that when the higher modes are isolated the input trace is truncated before the arrival of the fundamental mode. It will therefore be more important to ensure that there is sufficient frequency rejection.

APPENDIX C

Derivation of Two-Point Operators for Phase Velocity Filtering

The problem is to develop a set of one-dimensional space and time filter operators which will have the effect of attenuating all phase velocities outside a certain range. The two-point system is derived in a paper by Foster, Sengbush and Watson (1964) using a statistical technique. The approach adopted here will be essentially the same as that used in a paper by Embree et al. (1963) on the "pie-slice" process.

Suppose that it is required to pass phase velocities in the range $c'\Delta x/\Delta t$ where $c_1 < c' < c_2$; the appropriate space-time operators are found by performing the complex double Fourier transform

$$h(t,x) = \int_{-\infty}^{+\infty} e^{2\pi i \bar{f} t/\Delta t} \left(\int_{\bar{f}/c_2}^{\bar{f}/c_1} e^{2\pi i \bar{k} x/\Delta x} \, d\bar{k} \right) d\bar{f} \qquad \text{(C.1)}$$

Δx and Δt are the sampling distance and time; $\bar{f} = f\Delta t$, $\bar{k} = k\Delta x$ where f and k are frequency and wave number. In order to make the problem symmetrical the following changes of variable are made:

$$\begin{aligned} \bar{k} &= \bar{k}' - \frac{\bar{f}}{c}\left(\frac{1}{c_1} + \frac{1}{c_2}\right) \\ \frac{1}{c} &= \frac{1}{2}\left(\frac{1}{c_1} - \frac{1}{c_2}\right) \\ t' &= t + \frac{\Delta t}{2}\left(\frac{1}{c_1} + \frac{1}{c_2}\right)\frac{x}{\Delta x} \end{aligned} \qquad \text{(C.2)}$$

and hence equation (C.1) becomes

$$h'(t',x) = \int_{-\infty}^{+\infty} e^{2\pi i \bar{f}\, t/\Delta t}\left(\int_{-\bar{f}/c}^{+\bar{f}/c} e^{2\pi i \bar{k} x/\Delta x}\, d\bar{k}\right) d\bar{f} \qquad \text{(C.3)}$$

For a digital system in which time and space are sampled at increments Δt and Δx the frequency-wave number characteristics are periodic over the interval $-1/2 \leqslant \bar{f}, \bar{k} \leqslant +1/2$ (see Appendix D), so that the frequency integral is only taken over the range $\pm 1/2$; furthermore, let

$$\left.\begin{aligned} x_m &= \left(M + \tfrac{1}{2}\right)\Delta x \\ t'_{N'} &= \left(N' + \tfrac{1}{2}\right)\Delta t \end{aligned}\right\} \quad M, N' \text{ are integers}$$

The necessity for x_M not to be zero is revealed as the derivation progresses. Equation (C.3) becomes

$$h'(t'_{N'}, x_M) = \int_{-\frac{1}{2}}^{+\frac{1}{2}} e^{2\pi i \bar{f}(N'+\frac{1}{2})} \left(\int_{-\bar{f}/c}^{+\bar{f}/c} e^{2\pi i \bar{k}(M+\frac{1}{2})} \, d\bar{k} \right) d\bar{f}$$

and since $\sin 2\pi(\bar{f}/c)(m + 1/2)$ is an odd function of $\bar{f}$,

$$h'(t'_{N'}, x_M) = \frac{2i}{\pi(M+\frac{1}{2})} \int_0^{\frac{1}{2}} \sin\left[2\pi \frac{\bar{f}}{c}(M+\tfrac{1}{2})\right] \sin\left[2\pi \bar{f}(N'+\tfrac{1}{2})\right] d\bar{f}$$

$$= \frac{2i}{\pi(M+\frac{1}{2})} \int_0^{\frac{1}{2}} \left[\cos 2\pi \bar{f}\left(N'+\tfrac{1}{2}+(M+\tfrac{1}{2})\tfrac{1}{c}\right) - \cos 2\pi \bar{f}\left(N'+\tfrac{1}{2}-(M+\tfrac{1}{2})\tfrac{1}{c}\right) \right] d\bar{f}$$

$$= \frac{i}{\pi(M+\frac{1}{2})} \left\{ \frac{\sin \pi\left[N'+\frac{1}{2}+(M+\frac{1}{2})\frac{1}{c}\right]}{N'+\frac{1}{2}+(M+\frac{1}{2})\frac{1}{c}} - \frac{\sin \pi\left[N'+\frac{1}{2}-(M+\frac{1}{2})\frac{1}{c}\right]}{N'+\frac{1}{2}-(M+\frac{1}{2})\frac{1}{c}} \right\} \qquad \text{(C.4)}$$

In order that the expression inside the sine term be an integer, let $c = 1/p$ where p is an odd integer. Then the set of operators given by equation (C.4) has non-zero values only when $N' = -p(M + 1/2) - 1/2,\ p(M + 1/2) - 1/2$; when the values are $\pm i/(\pi(M + 1/2))$ respectively. The fact that

the operators are imaginary implies that in the original Fourier double integral, equation (C.1), the sine transform is the only part that contributes. The original phase velocity filtering is obtained by making the following changes of variable:

$$N' = N + \frac{1}{2}\left(\frac{1}{c_1} + \frac{1}{c_2}\right)\left(M + \frac{1}{2}\right) \qquad \text{(C.5)}$$

corresponding to $t' = t + \frac{\Delta t}{2}\left(\frac{1}{c_1} + \frac{1}{c_2}\right) x/\Delta x$, with the requirement that $1/2\left(\frac{1}{c_1} + \frac{1}{c_2}\right)$ be an even integer so that the time shifts correspond to multiples of the sampling interval Δt. Thus the conditions imposed on the two-point time domain sampling process are, from (C.2) and (C.5),

$$\frac{1}{2}\left(\frac{1}{c_1} - \frac{1}{c_2}\right) = p \quad \text{(odd integer)}$$

$$\frac{1}{2}\left(\frac{1}{c_1} + \frac{1}{c_2}\right) = q \quad \text{(even integer)} \qquad \text{(C.6)}$$

In the frequency wave number domain the required rejection is obtained by multiplying the filter set with the trace

set; in the space-time domain this is equivalent to a double convolution (Lee, 1960) and for the digital case the filtered traces are

$$p_o(x_M, t_N) = \sum_{M'} \sum_{N'} p_i(x_{M-M'}, t_{N-N'})\, h(x_{M'}, t_{N'}) \qquad \text{(C.7)}$$

where $p_o(x_M, t_N)$ refers to output trace at $x_M = M\Delta x$, $p_i(x_{M-M'}, t_{N-N'})$ refers to input trace at $x_{M-M'} = (M - M' + 1/2)\Delta x$, and $h(x_{M'}, t_{N'})$ is the set of two-point time domain operators. The filtered trace corresponding to the center of the array at x = 0 is given by putting M = 0 in equation (C.7), to give

$$p_o(x_0, t_N) = \sum_{M'} \sum_{N'} p_i(x_{0-M'}, t_{N-N'})\, h(x_{M'}, t_{N'}) \qquad \text{(C.8)}$$

where

$$h(x_{M'}, t_{N'}) = \frac{1}{\pi(M'+\frac{1}{2})}\left[\delta\left\{N'+\tfrac{1}{2}\left(\tfrac{1}{C_1}+\tfrac{1}{C_2}\right)\left(M'+\tfrac{1}{2}\right)\right\} - \delta\left\{N'-\tfrac{1}{2}\left(\tfrac{1}{C_1}+\tfrac{1}{C_2}\right)\left(M'+\tfrac{1}{2}\right)\right\}\right]$$

One point should be noted, that the time reference for the output trace t_N is not the same as that for the input trace, causing constant phase shifts in the frequency components. However, in deriving phase velocities only phase changes for each frequency component are considered, so that this shift is not important.

The above analysis is so far exact; the only condition imposed now is that the number of space samples be limited to 2M, multiplying the exact set of operators by a finite series of periodic impulses

$$U(x) = \sum_{m=-(M+\frac{1}{2})}^{m=+(M+\frac{1}{2})} \delta(x - m\Delta x) \qquad \text{(C.9)}$$

which in the wave number domain is equivalent to convolving the Fourier transform of the operators with the Fourier transform of equation (C.9), which is

$$\begin{aligned} \overline{U}(\bar{k}) &= \frac{1}{\Delta x}\int_{-\infty}^{+\infty} U(x)\, e^{-2\pi i \bar{k} x/\Delta x}\, dx \\ &= \sum_{m=0}^{m=M} e^{2\pi i \bar{k}(m+\frac{1}{2})} + e^{-2\pi i \bar{k}(m+\frac{1}{2})} \\ &= \frac{SIN[2\pi\,\bar{k}(M+1)]}{SIN[\pi\,\bar{k}]} \end{aligned} \qquad \text{(C.10)}$$

This function is shown in Figure 15 for M = 4. For wavelengths of the order of the dimensions of the array for which $\bar{k} = 1/2(m+1)$ the phase velocities passed are no longer defined by the operators, since the finite array is not able to resolve wavelengths of this magnitude.

APPENDIX D

Aliasing and Averaging Effect of Finite Digital Sampling

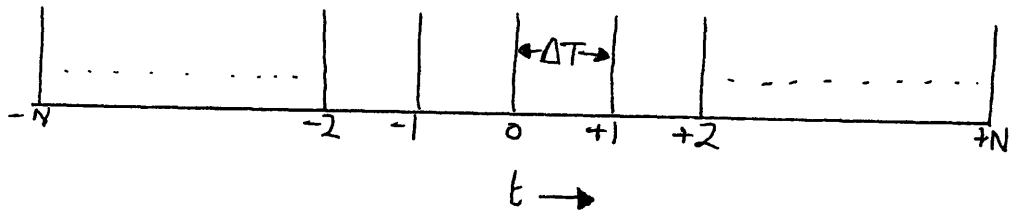

A finite digital system can be treated as a set N of equi-spaced unit impulses.

To make the time domain operators symmetrical so that the complex Fourier transform is real, a symmetrical set of impulses at negative times are added; these do not affect the analysis as the disturbance is zero outside the positive time region. The Fourier transform of such a set of impulses is

$$U(f) = \int_{-\infty}^{+\infty} \sum_{n=-N}^{n=+N} \delta(t - n\Delta T)\, e^{-2\pi i f t}\, dt$$

$$= 1 + \sum_{n=1}^{n=N} \left(e^{2\pi i f n \Delta t} + e^{-2\pi i f n \Delta t} \right)$$

$$= \frac{SIN[\pi(2N+1) f \Delta T]}{SIN[\pi f \Delta T]} \qquad \text{(D.1)}$$

Equation (D.1) is drawn in Figure 20 for N = 4. The effect of finite digital sampling on a signal is to convolve its Fourier transform with equation (D.1) which is periodic over the interval $1/\Delta T$. Negative frequencies have no physical meaning but are used to make the function symmetrical so that in taking the complex Fourier transform only the real cosine part contributes. Since real traces have zero amplitude in the negative frequency range, the effect of digital sampling is to restrict measurements to the frequency range zero to $1/\Delta T$.

Finite sampling introduces small side lobes and a central peak of half-width $1/(2N+1)\Delta T$, effectively restricting the useful sampling frequency to a minimum

$1/(2N+1)$ T for signals that extend beyond the range of sampling. However, for a transient signal wholly within this range of sampling no such restriction is imposed; it is this second assumption which is made for all experimental data.

Finally, the above analysis can be extended in an exactly similar fashion to space sampling, and the results derived are very similar with wave number and Δx replacing frequency and ΔT. In this case negative wave numbers have a real meaning and refer to direction of propagation of the disturbance in one dimension.

TABLE I

Description of Event and Recorded Traces

Origin time: June 12, 1960; 07^h 19' 43"

Approximate location of epicentre: 36°S, 98°W

Magnitude: 6½

Instrument: free period of pendulum = 80"

free period of galvanometer = 90"

PHASE	G1	G2	G3
Arrival time	07^h 47' 00"	09^h 10' 00"	10^h 13' 00"
Distance to Pasadena			
Uncorrected	8045 km	31960 km	48060 km
Corrected	8225 km	31780 km	48240 km
Length of trace	16'	20'	17'
Number of points	321	401	341
Digitization interval	3"	3"	3"

TABLE IIa

Phase Velocities for Fundamental Love Mode

Period (seconds)	Phase Velocity		
	G1 - G3	G2 - G3	G1 - G2
333.33	5.295	5.322	5.275
285.71	5.148	5.161	5.138
250.00	5.044	5.061	5.031
222.22	4.962	4.974	4.951
200.00	4.892	4.889	4.893
181.82	4.840	4.829	4.845
166.67	4.799	4.789	4.803
153.85	4.764	4.757	4.767
142.86	4.733	4.727	4.736
133.33	4.705	4.699	4.708
125.00	4.681	4.675	4.683
117.65	4.661	4.655	4.662
111.11	4.642	4.638	4.643
105.26	4.629	4.628	4.627
100.00	4.619	4.627	4.612
90.91	4.599	4.617	4.584
80.00	4.570	4.629	4.529
68.97	4.541	4.609	4.493
60.61	4.511	4.596	4.452
52.63	4.479	4.593	4.402
44.44	4.468	4.649	4.347

TABLE IIb

Phase Velocities for First Higher Love Mode

Period (seconds)	Phase Velocity		
	G1 - G3	G2 - G3	G1 - G2
173.91	6.559	6.585	6.540
166.67	6.434	6.427	6.438
160.00	6.325	6.303	6.338
153.85	6.228	6.200	6.248
148.15	6.141	6.104	6.165
142.86	6.063	6.021	6.090
137.93	5.992	5.948	6.022
133.33	5.928	5.881	5.959
129.03	5.869	5.821	5.901
125.00	5.814	5.766	5.847
121.21	5.764	5.716	5.797
117.65	5.718	5.670	5.750
111.11	5.634	5.591	5.663
105.26	5.561	5.525	5.584
100.00	5.494	5.461	5.515
95.24	5.428	5.385	5.456
90.91	5.370	5.318	5.406
85.11	5.303	5.246	5.342
75.47	5.189	5.109	5.244

TABLE IIc

Phase Velocities for Second Higher Love Mode

Period (seconds)	Phase Velocity		
	G1 - G3	G2 - G3	G1 - G2
95.24	6.625	6.839	6.435
90.91	6.478	6.623	6.331
86.96	6.349	6.442	6.238
83.33	6.235	6.294	6.147
80.00	6.134	6.168	6.063
74.07	5.964	5.975	5.909
68.97	5.826	5.836	5.773
64.52	5.709	5.699	5.671
58.82	5.563	5.513	5.553
54.05	5.452	5.358	5.475
50.00	5.357	5.247	5.391
45.45	5.255	5.157	5.282
40.82	5.153	5.069	5.171

RELATIVE DISPLACEMENT WITH DEPTH FOR LOVE MODES AT 50 SEC PERIOD

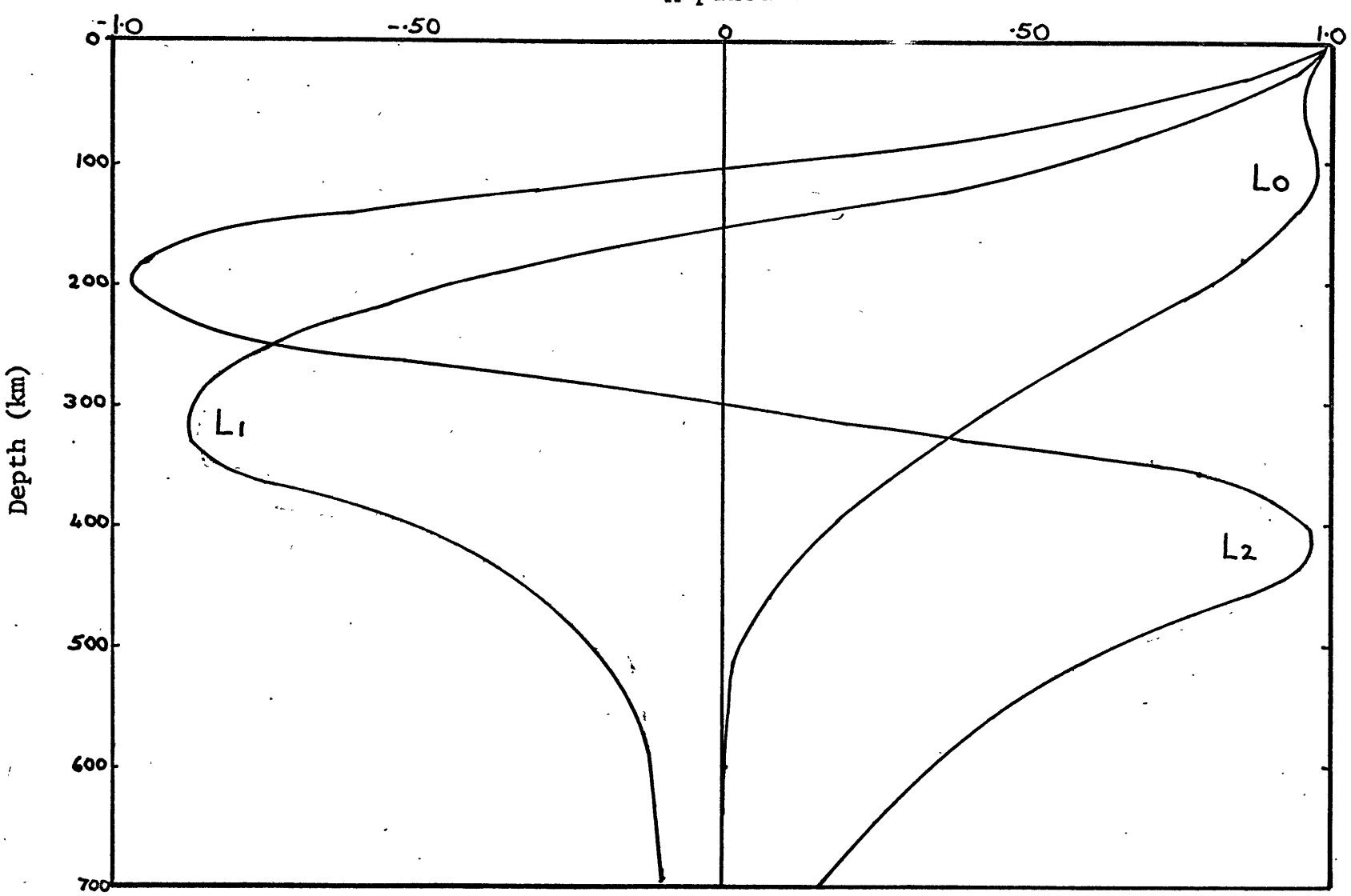

FIGURE 1

FIGURE 2

SHEAR VELOCITY WITH DEPTH FOR AN OCEANIC AND SHIELD MODEL

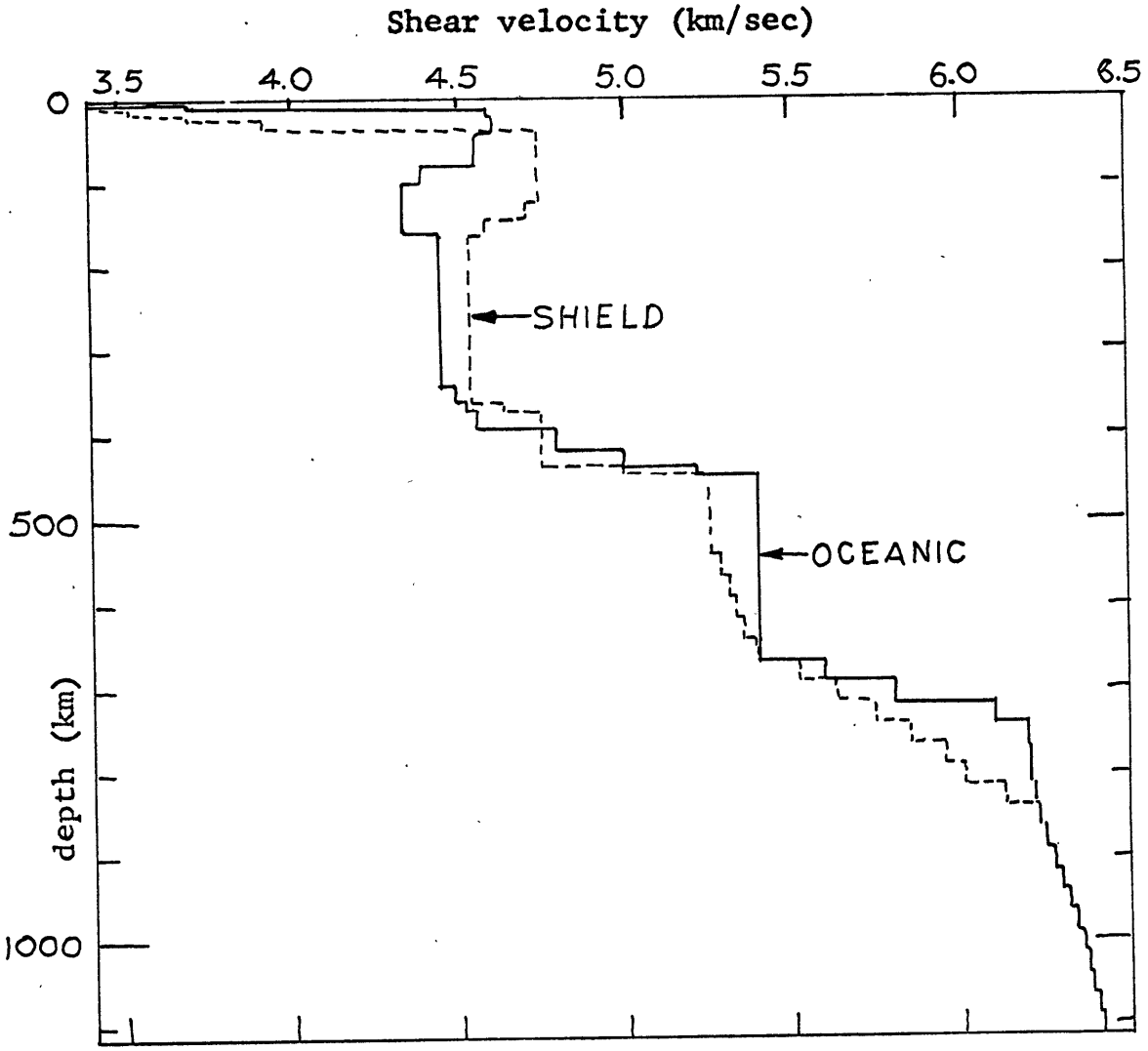

FIGURE 3

SLIDING FILTERS FOR LOVE MODES

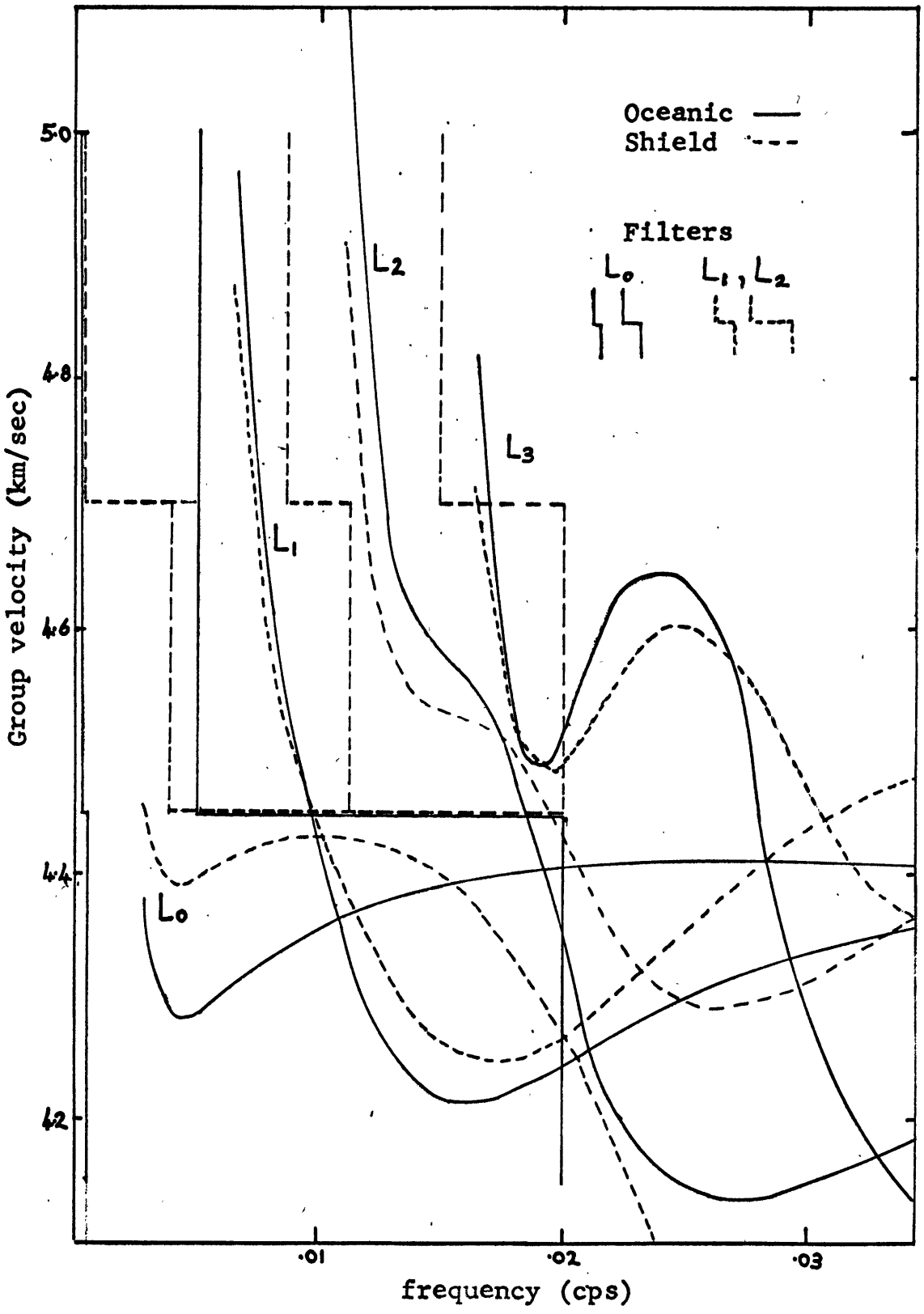

GREAT CIRCLE PATH FOR EVENT

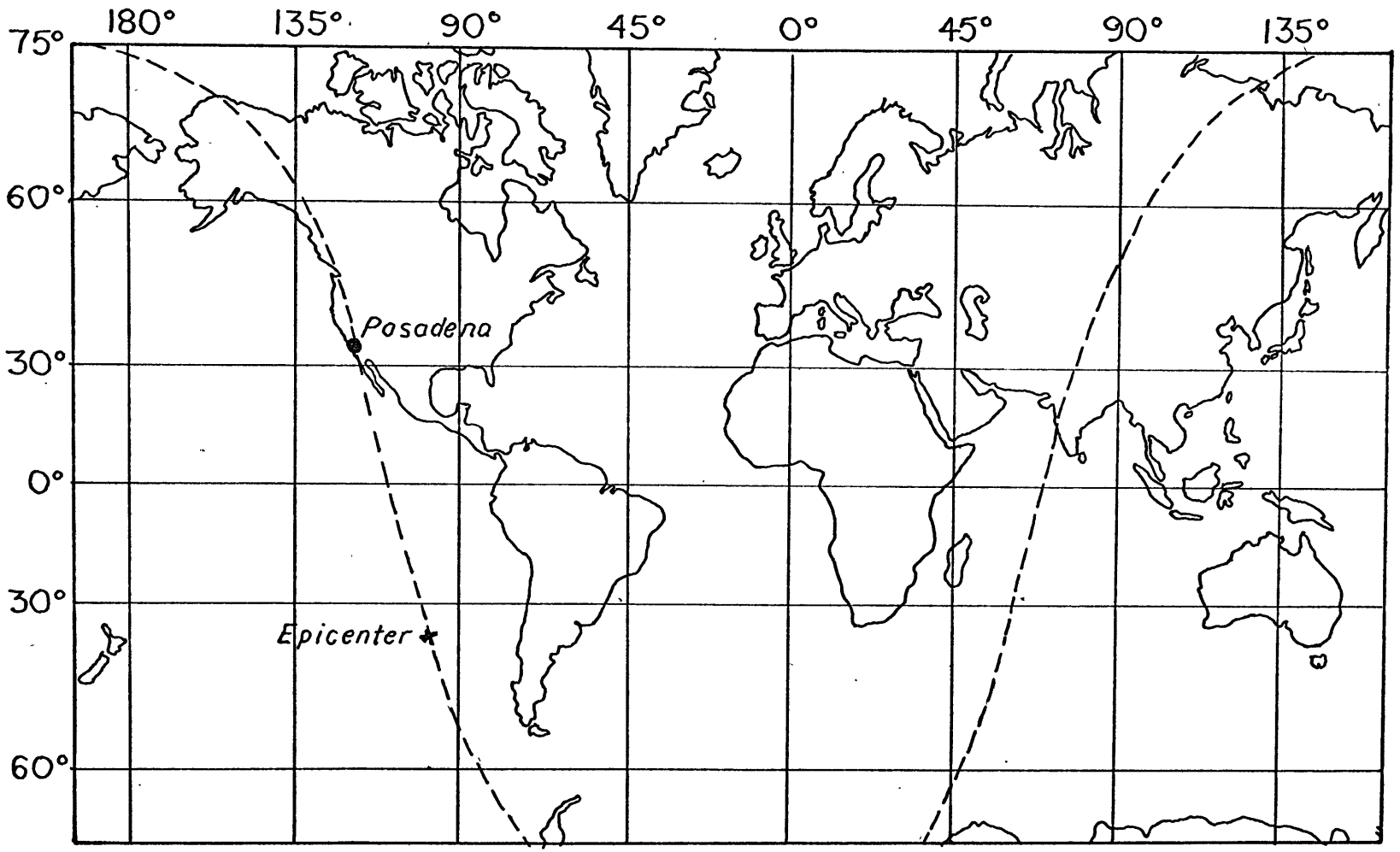

FIGURE 4

FIGURE 5a

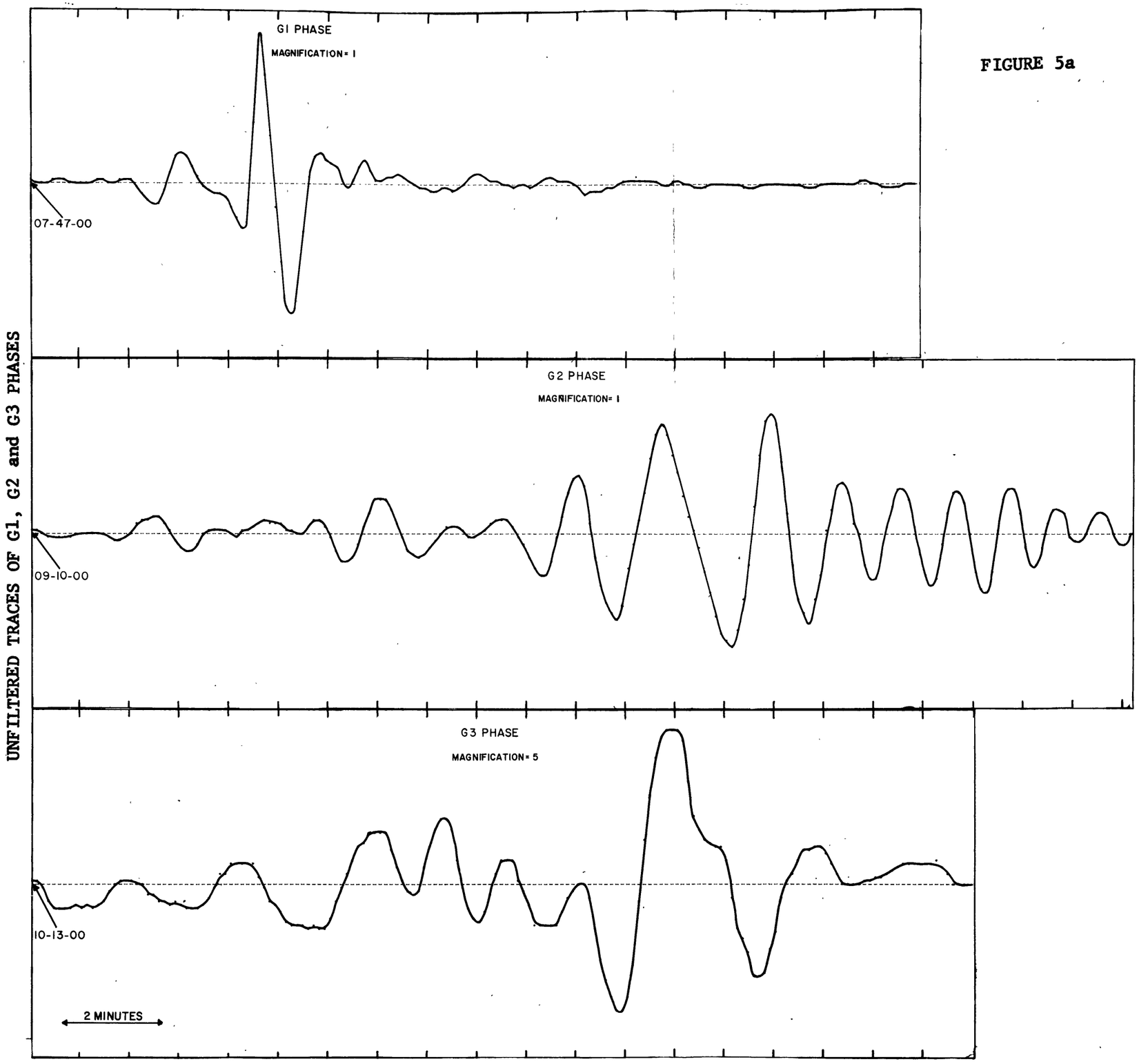
UNFILTERED TRACES OF G1, G2 and G3 PHASES
G1 PHASE
MAGNIFICATION= 1
07-47-00
G2 PHASE
MAGNIFICATION= 1
09-10-00
G3 PHASE
MAGNIFICATION= 5
10-13-00
2 MINUTES

FIGURE 5b

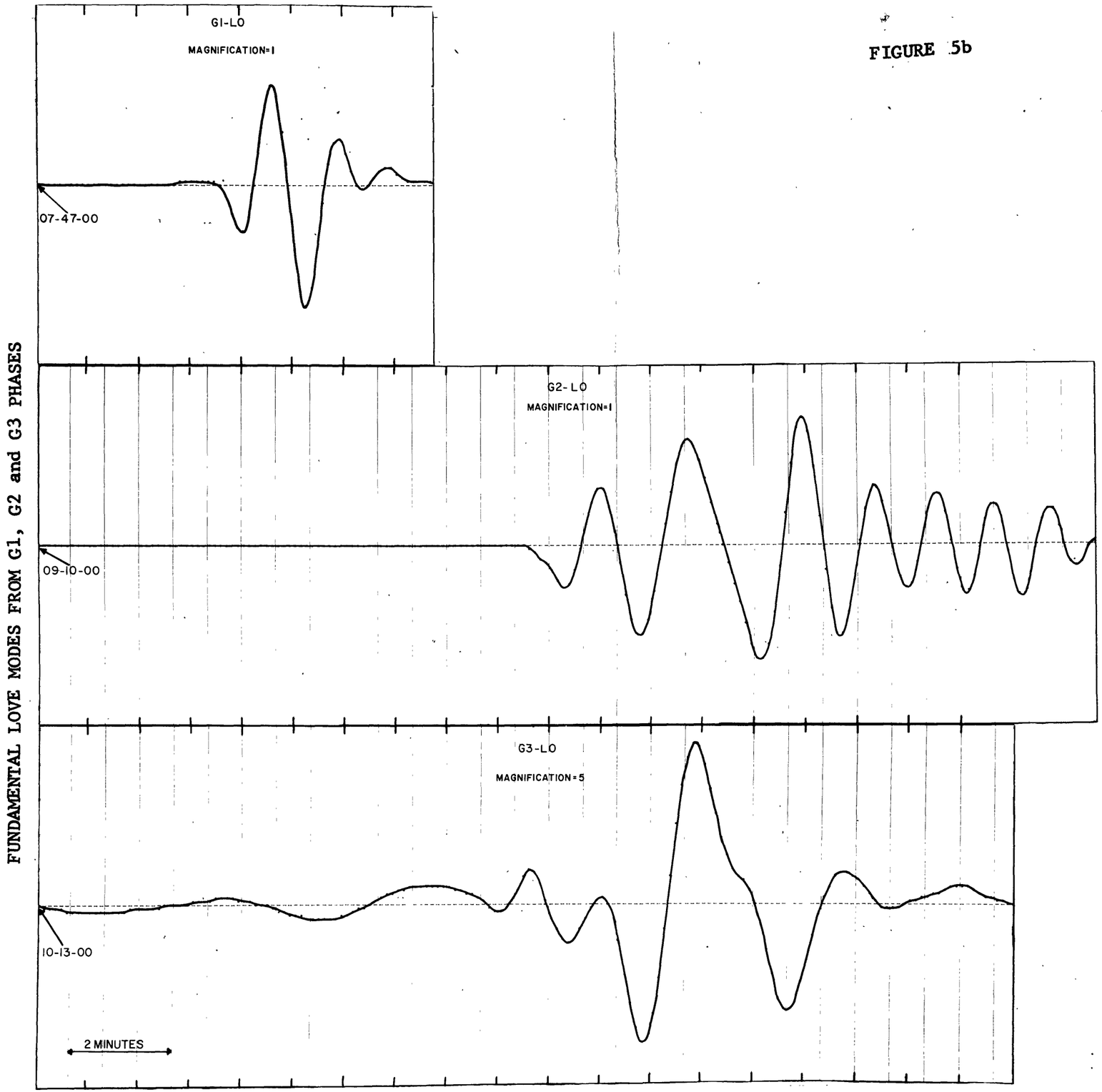
FUNDAMENTAL LOVE MODES FROM G1, G2 and G3 PHASES
G1-LO
MAGNIFICATION=1
07-47-00
G2-LO
MAGNIFICATION=1
09-10-00
G3-LO
MAGNIFICATION=5
10-13-00
2 MINUTES

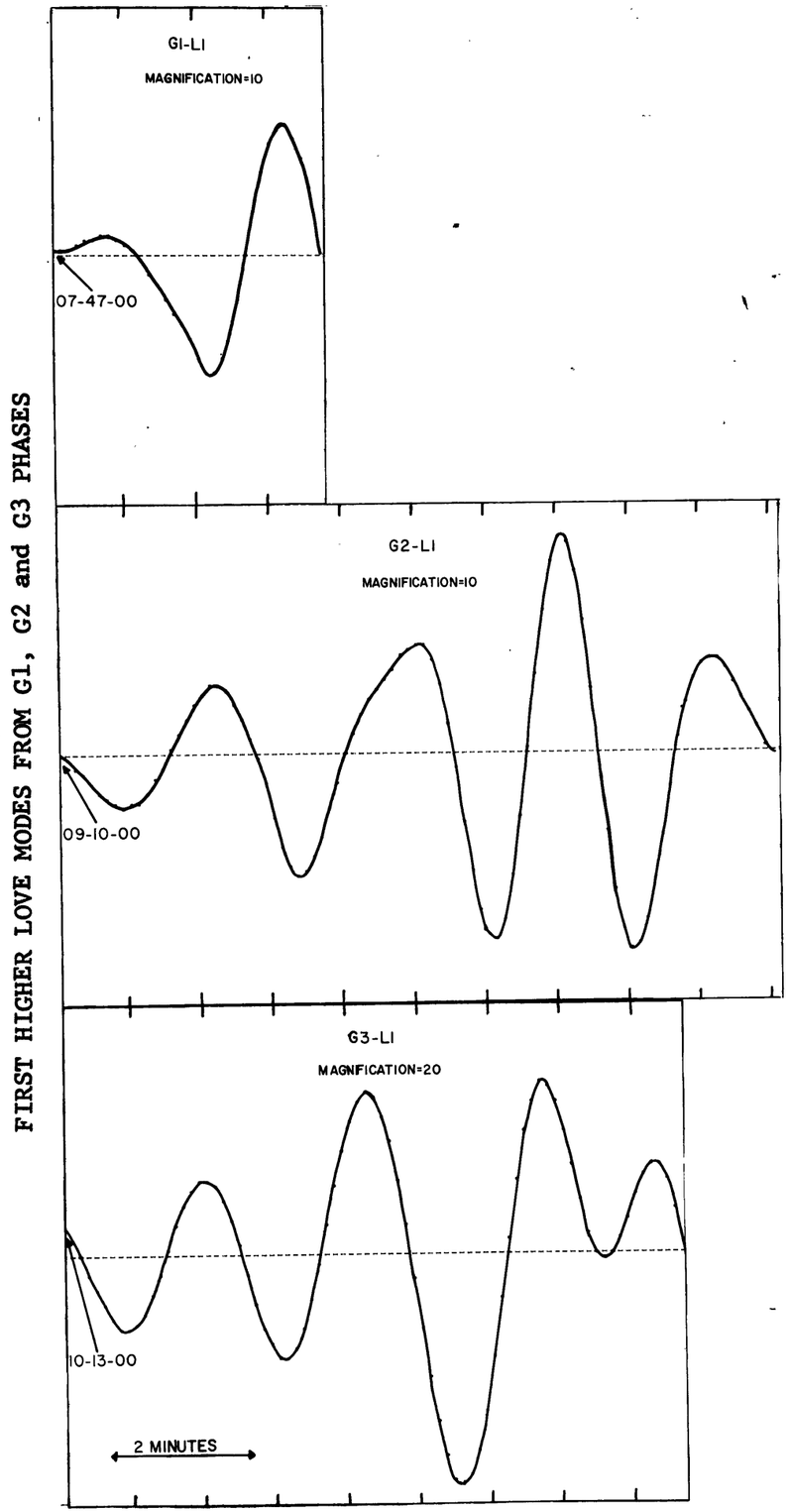
FIRST HIGHER LOVE MODES FROM G1, G2 and G3 PHASES
G1-L1
MAGNIFICATION=10
07-47-00
G2-L1
MAGNIFICATION=10
09-10-00
G3-L1
MAGNIFICATION=20
10-13-00
2 MINUTES

FIGURE 5c

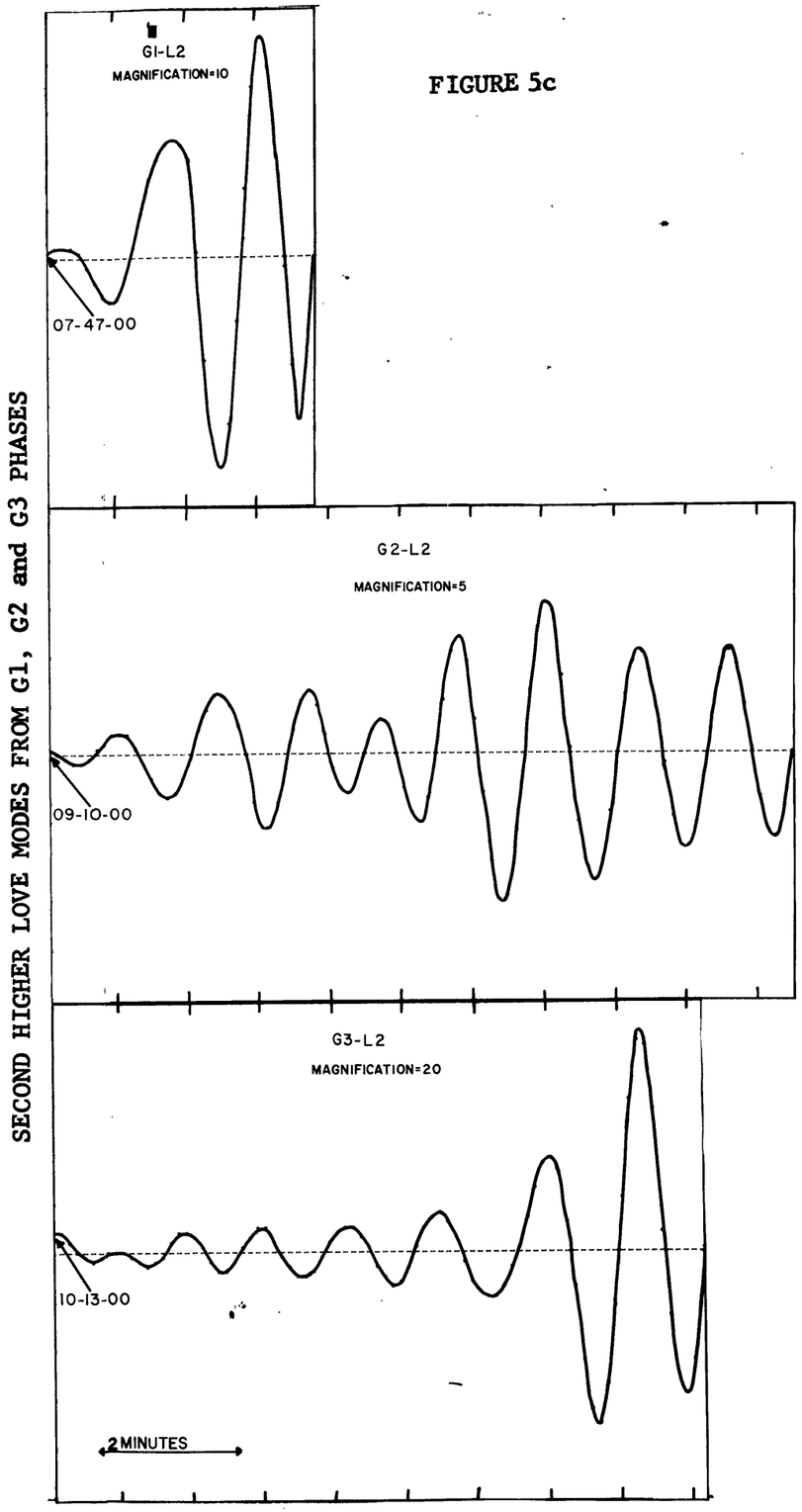
SECOND HIGHER LOVE MODES FROM G1, G2 and G3 PHASES
G1-L2
MAGNIFICATION=10
07-47-00
G2-L2
MAGNIFICATION=5
09-10-00
G3-L2
MAGNIFICATION=20
10-13-00
2 MINUTES

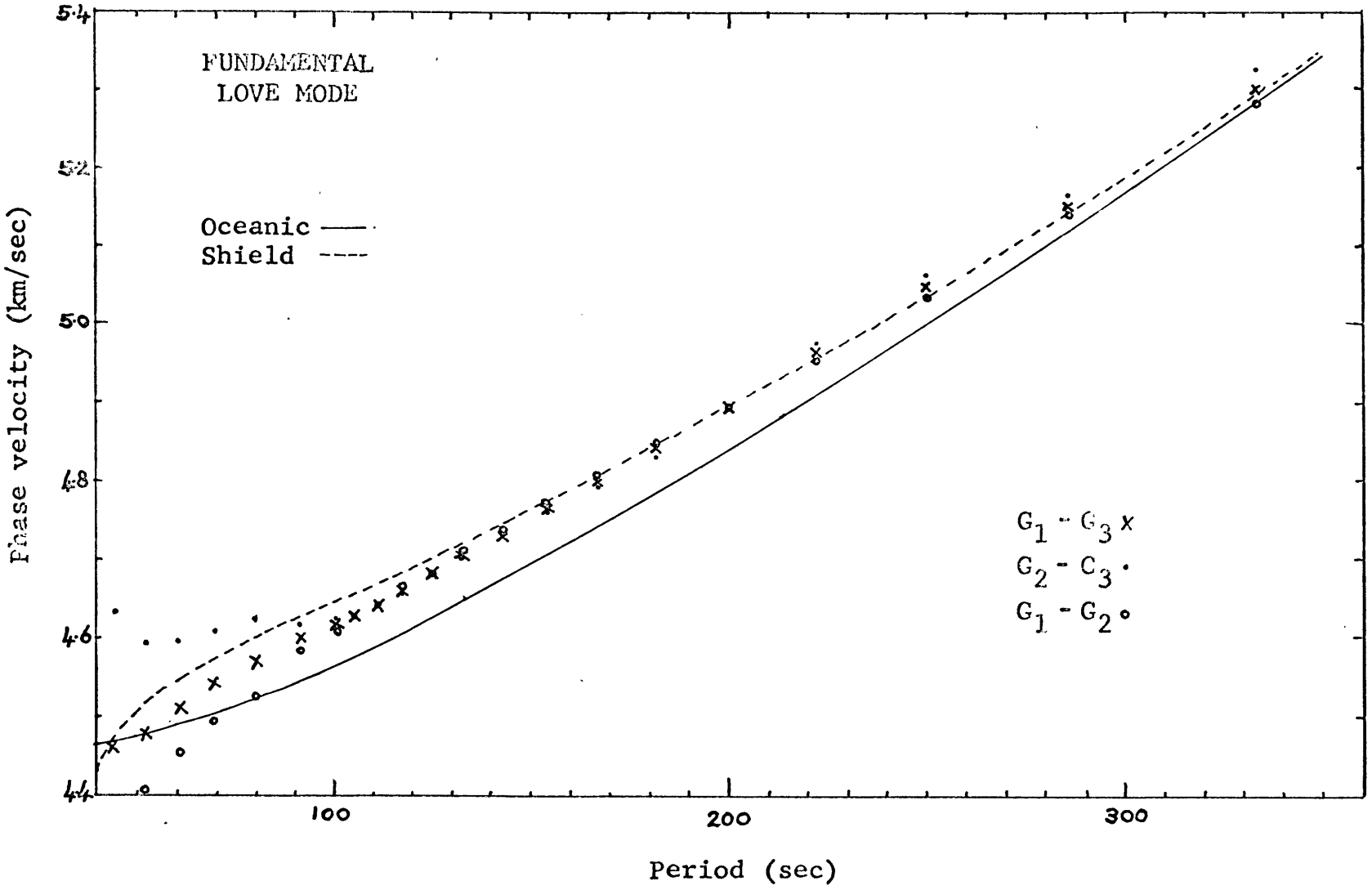
FUNDAMENTAL
LOVE MODE
Oceanic
Shield
$G_1 - G_3$ x
$G_2 - C_3$ •
$G_1 - G_2$ °
Phase velocity (km/sec)
5·4
5·2
5·0
4·8
4·6
4·4
100
200
300
Period (sec)

FIGURE 6

FIGURE 7

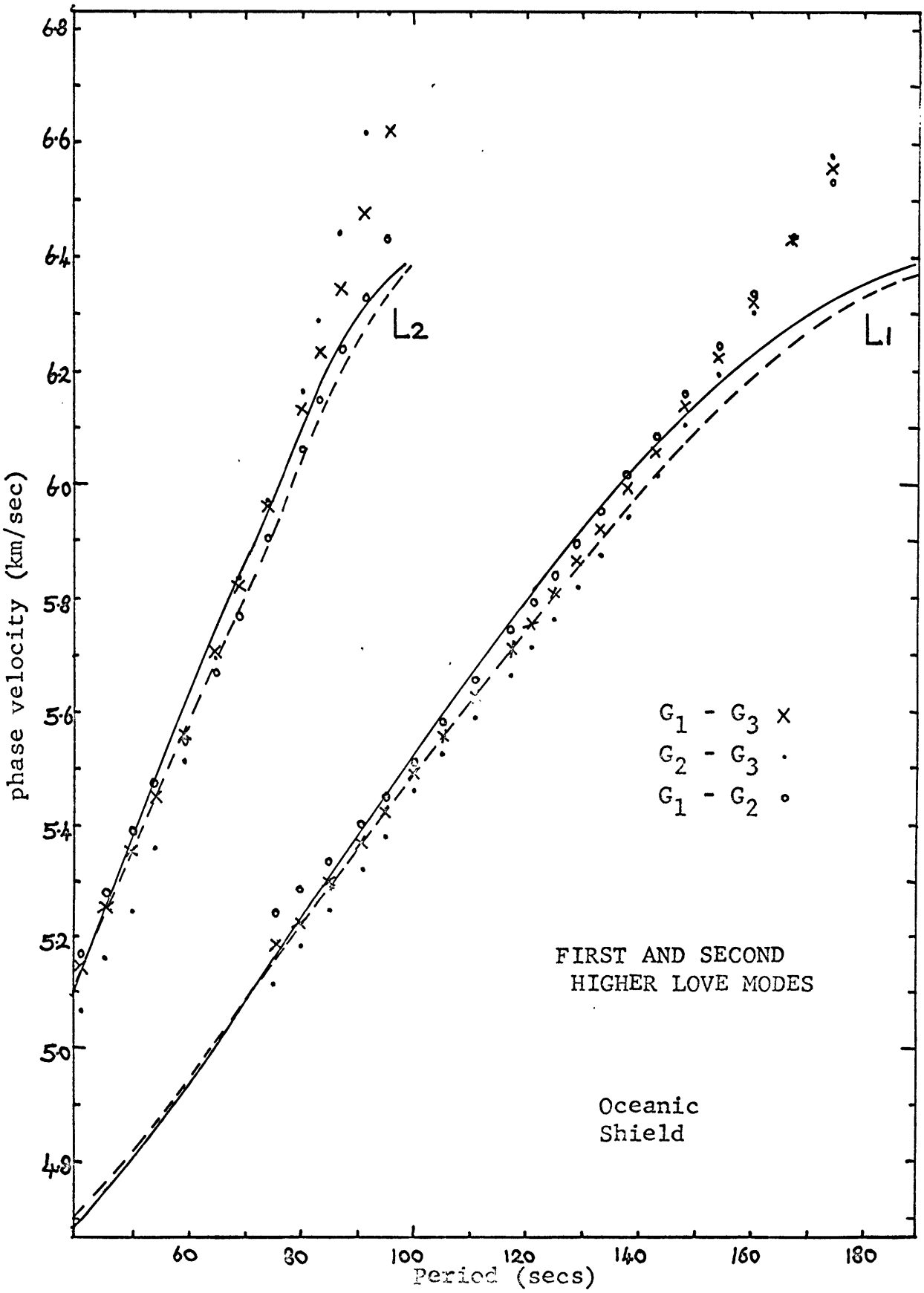
6·8
6·6
6·4
6·2
6·0
5·8
5·6
5·4
5·2
5·0
4·8
phase velocity (km/sec)
60
80
100
120
140
160
180
Period (secs)
L2
L1
G1 - G3 ×
G2 - G3 ·
G1 - G2 °
FIRST AND SECOND
HIGHER LOVE MODES
Oceanic
Shield

MODEL

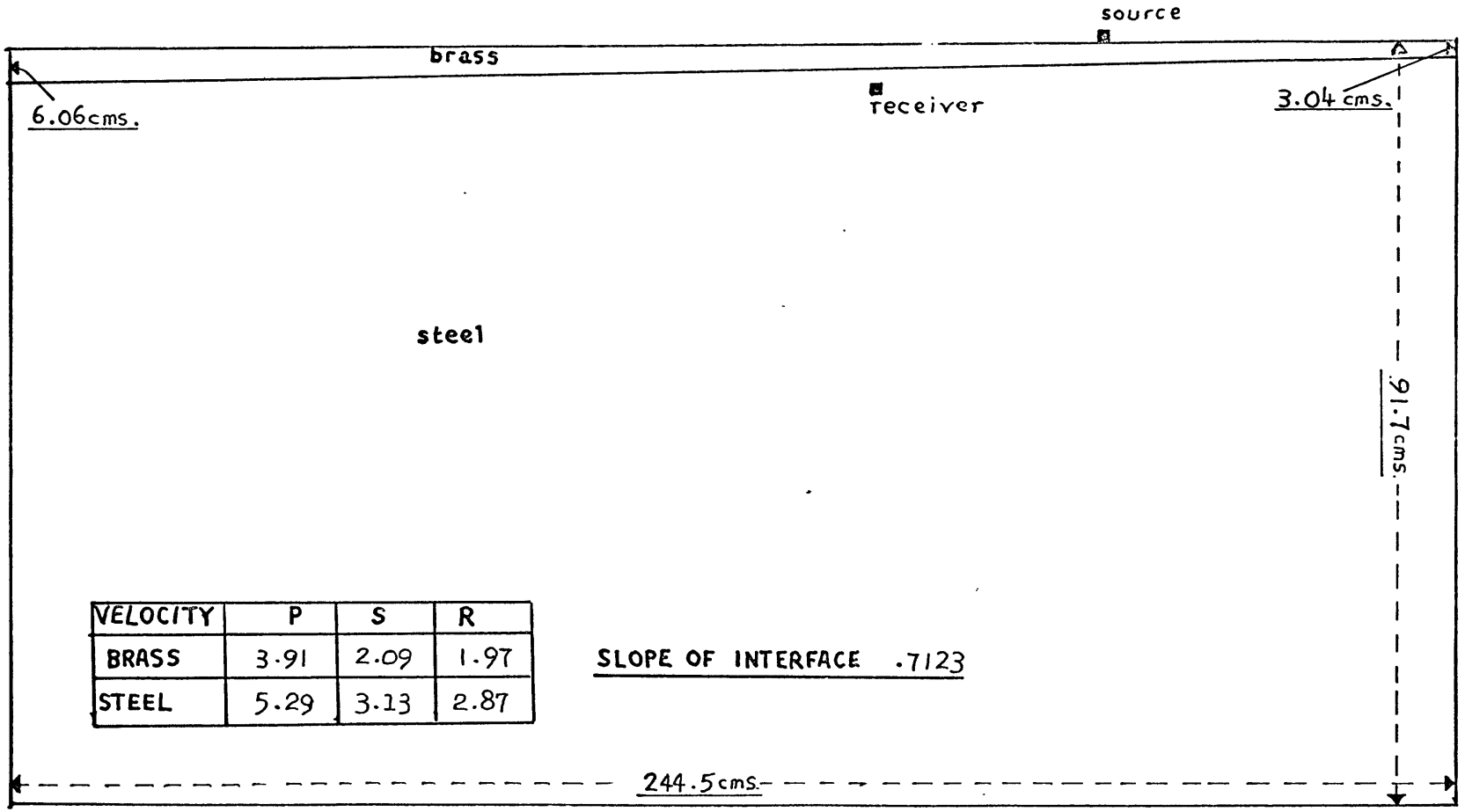

VELOCITY	P	S	R
BRASS	3.91	2.09	1.97
STEEL	5.29	3.13	2.87

SLOPE OF INTERFACE .7123

FIGURE 8

DISPERSION CURVE FOR MODEL WITH 4-CM BRASS LAYER

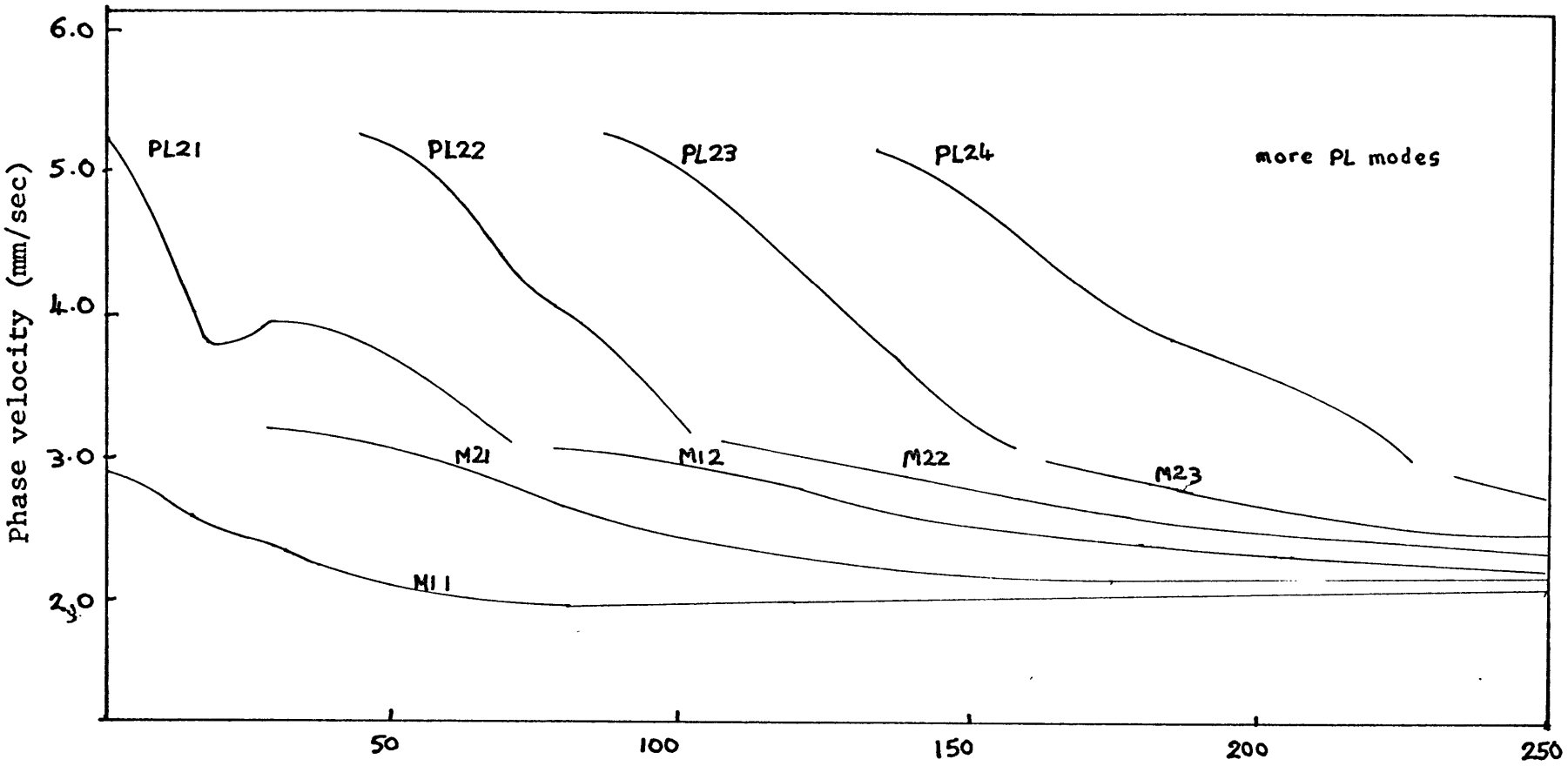

FIGURE 9

TWO POINT OPERATOR SET USED FOR PHASE VELOCITY FILTERING

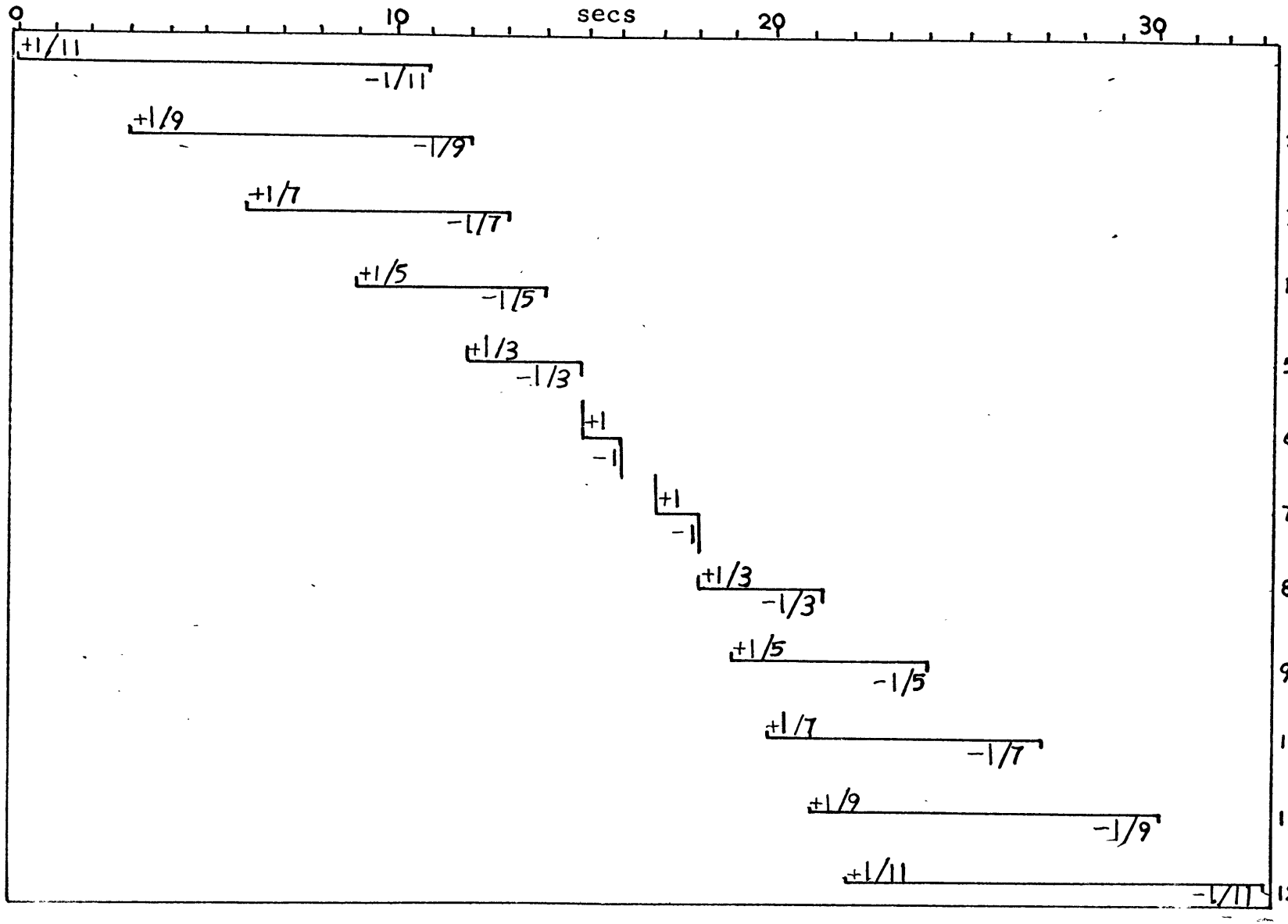

FIGURE 10.

FIGURE 11

FREQUENCY-WAVE NUMBER RESPONSE FOR 12-CHANNEL TWO-POINT OPERATOR SET

PASS BAND 10 mm/μsec - 3.[illegible] m / μsec

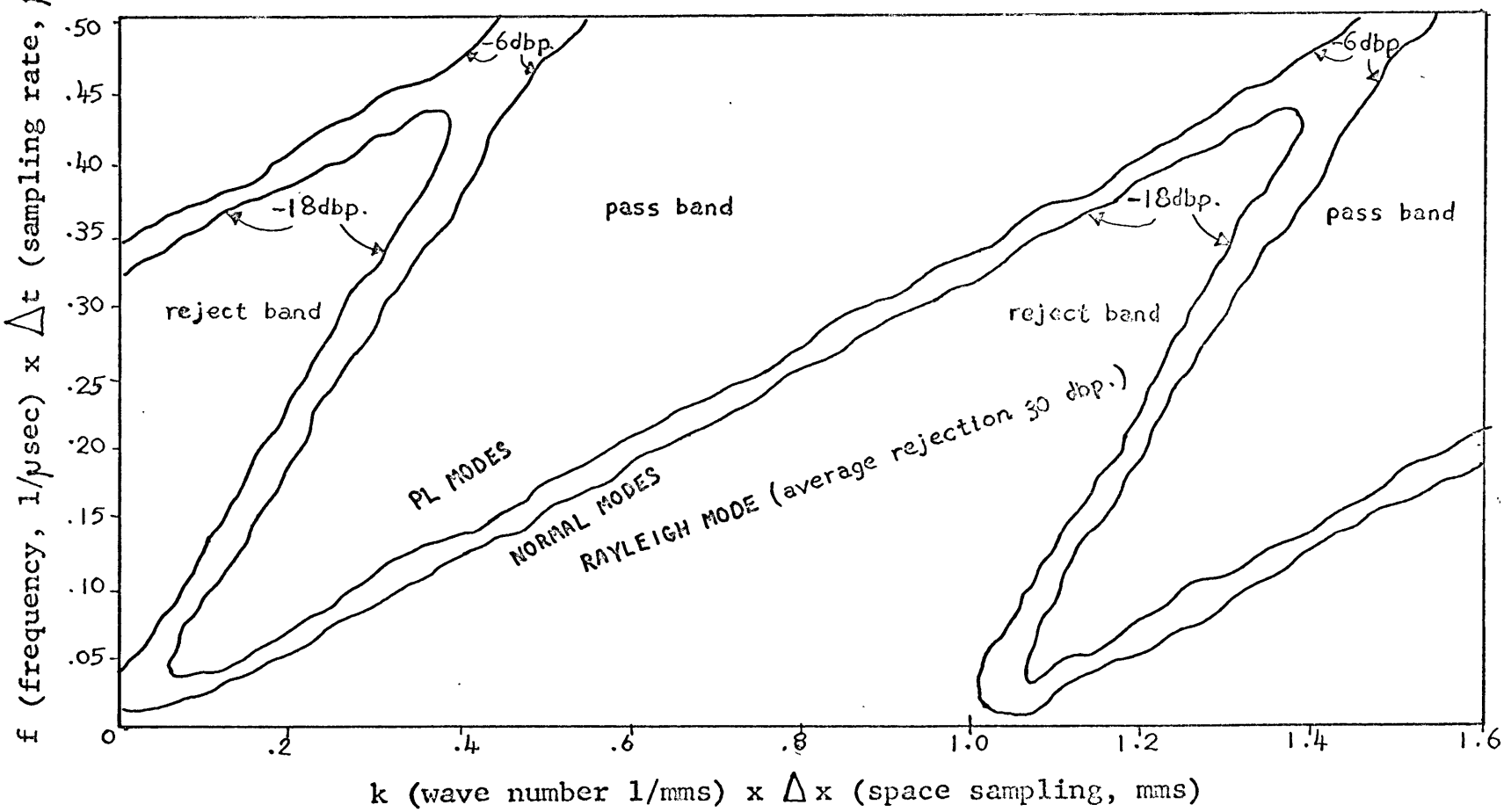

FIGURE 12

FILTERED AND UNFILTERED TRACES
AT A DISTANCE OF 285 mm FROM SOURCE

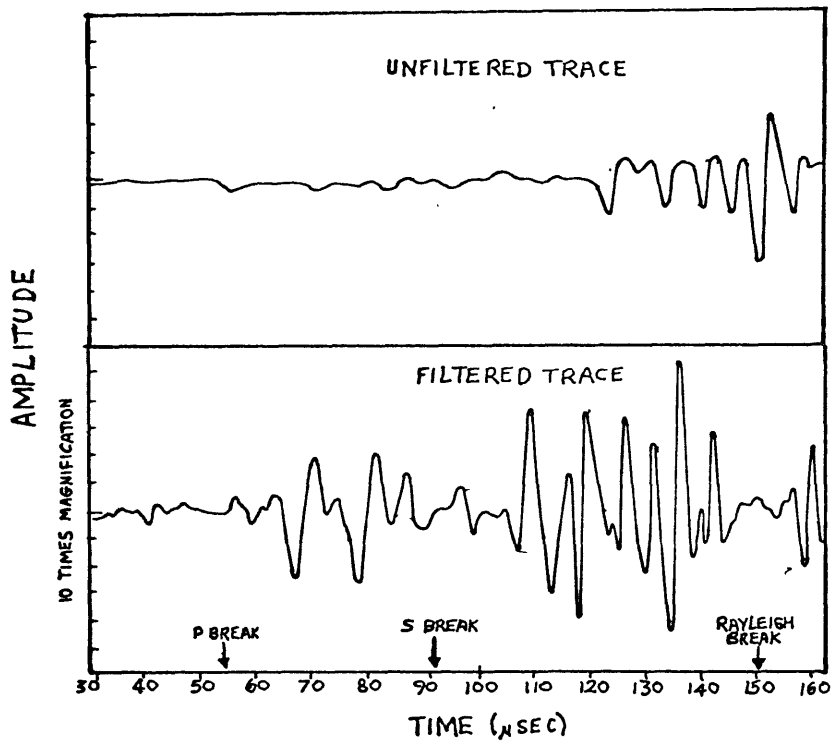

DISPERSION CURVES FROM A 50-POINT FILTER OPERATOR

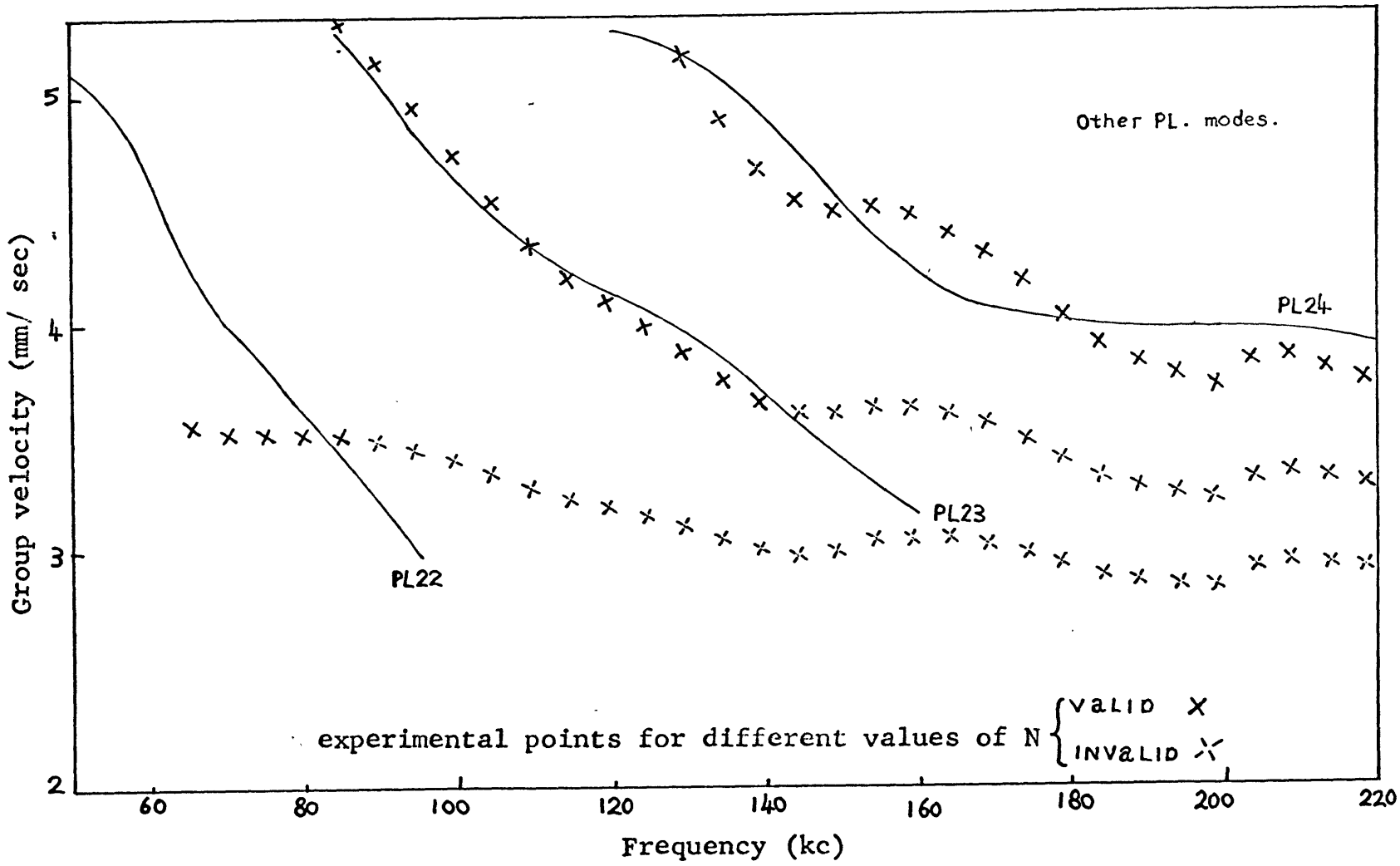

FIGURE 13

FIGURE 14

(a)

LASA ARRAY

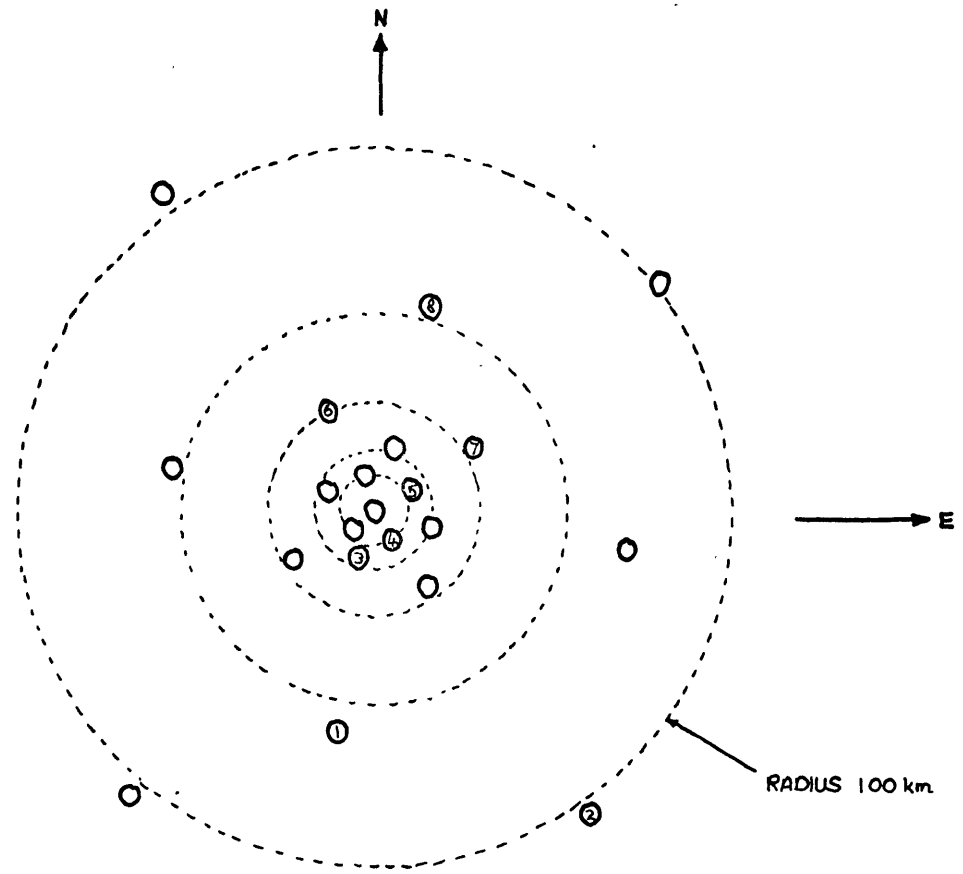

(b)

POSSIBLE LINEAR ARRAY FROM LASA

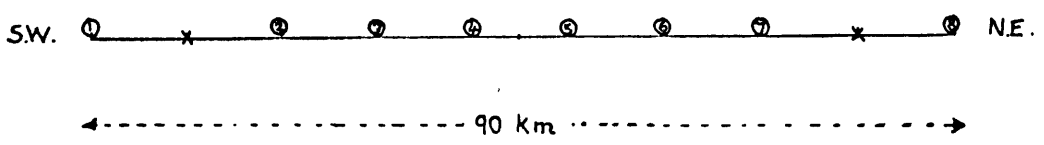

FIGURE 15

FOURIER TRANSFORM OF SAMPLING OPERATOR FOR LASA ARRAY

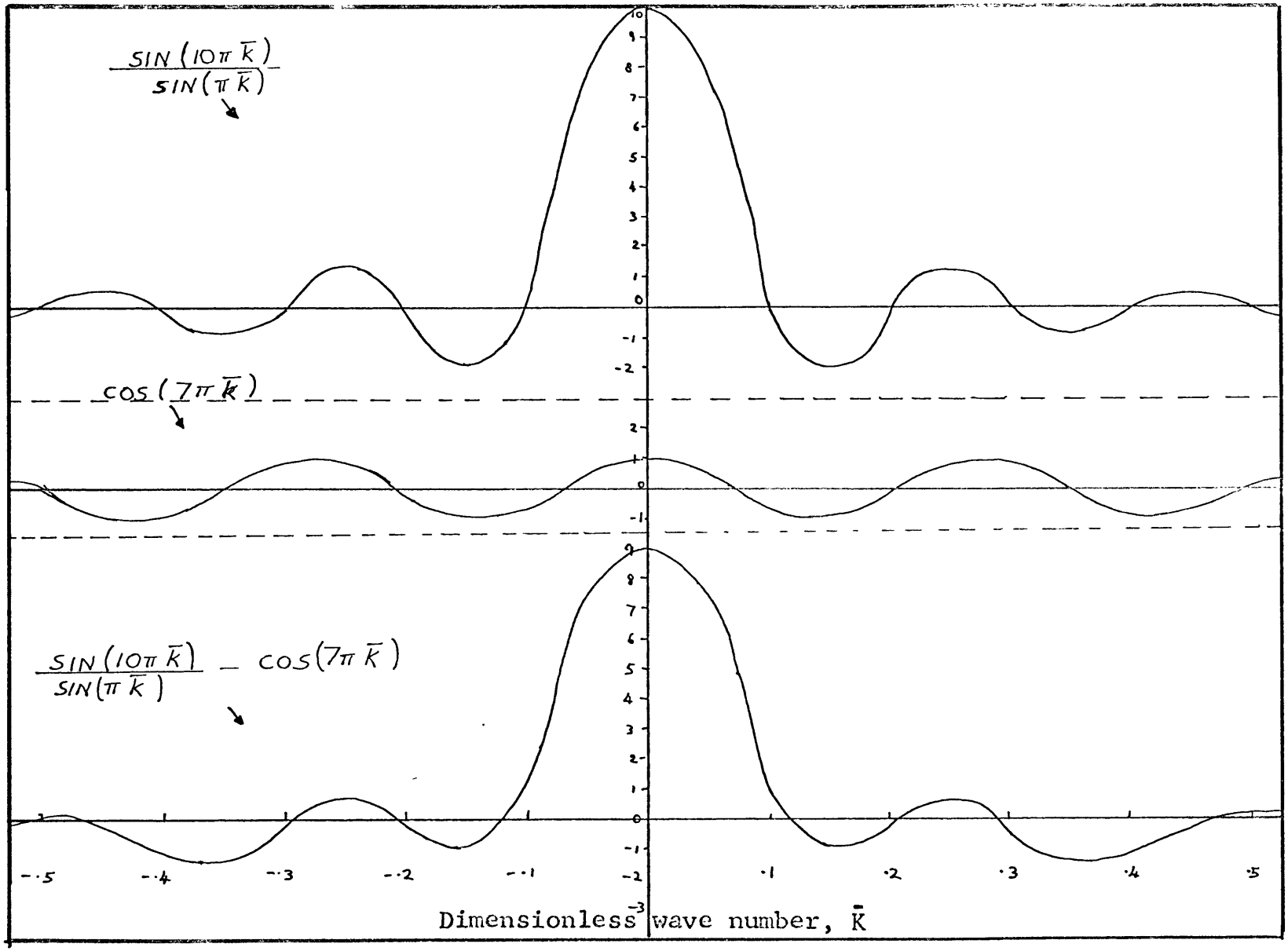

FIGURE 16

SOURCE PULSE GENERATED BY PIEZOELECTRIC CRYSTAL

Acoustical source pulse

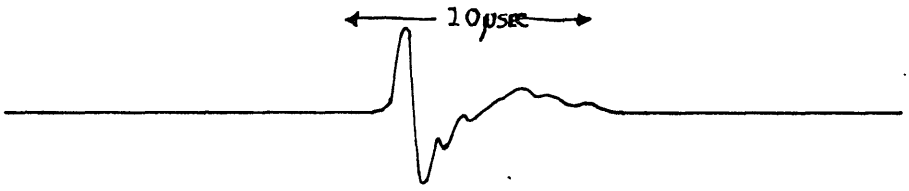

generated by rectangular electrical input to crystal

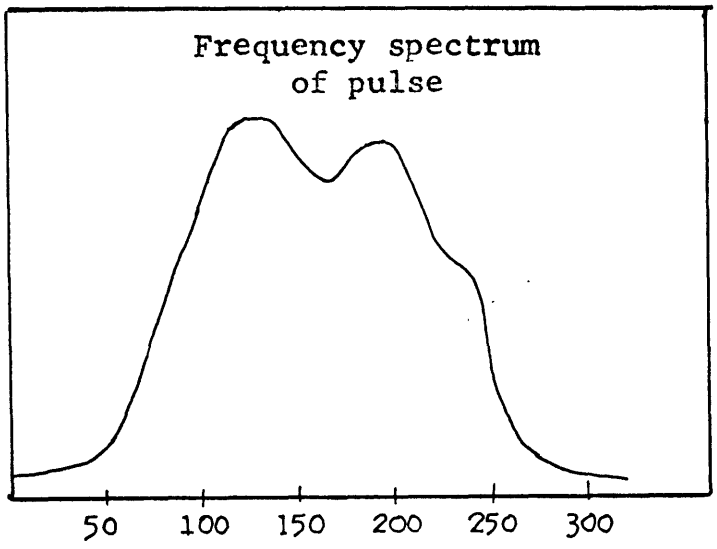

FIGURE 17

THEORETICAL GROUP VELOCITY FOR PL MODES

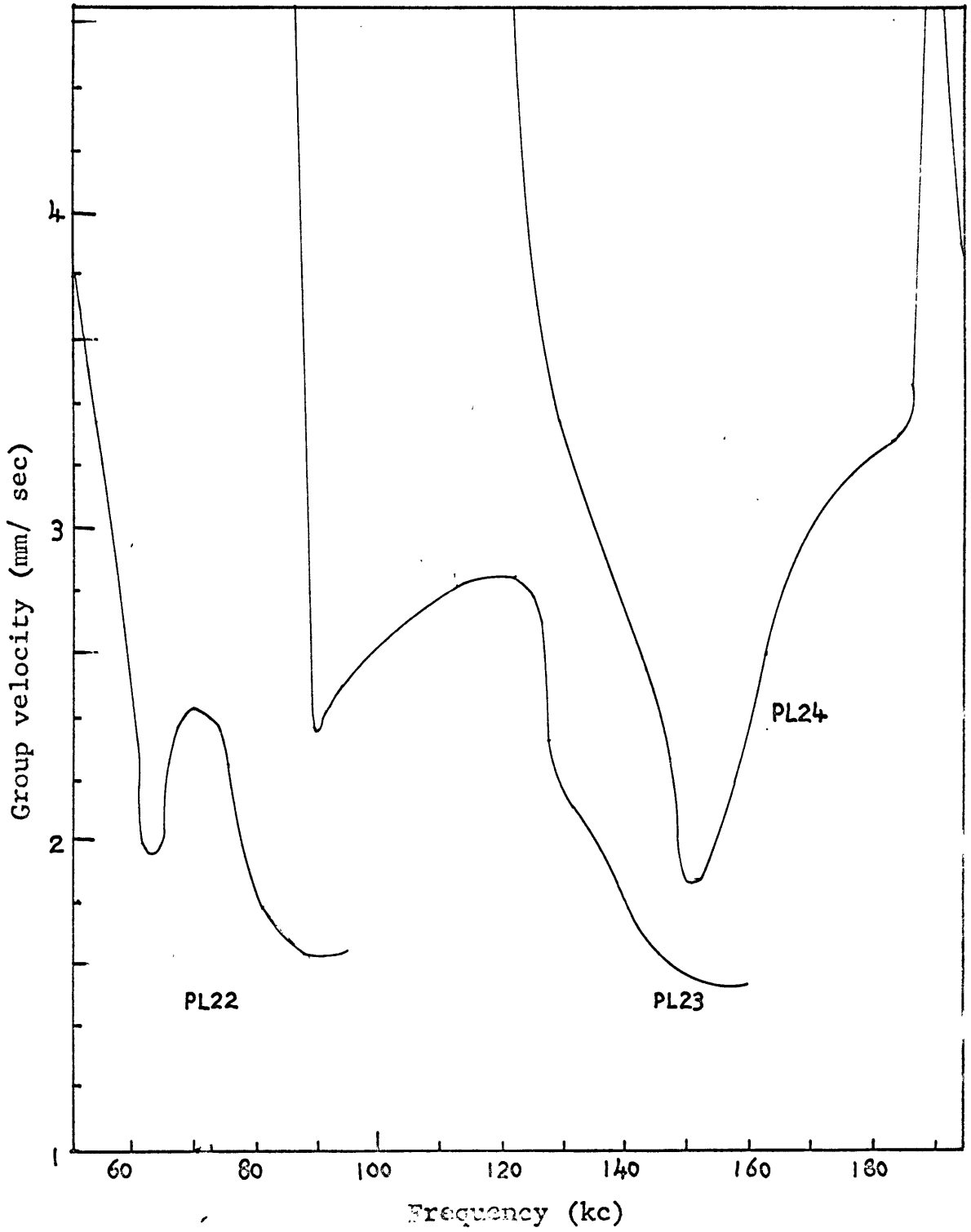

FIGURE 18

THEORETICAL ATTENUATION FOR PL MODES

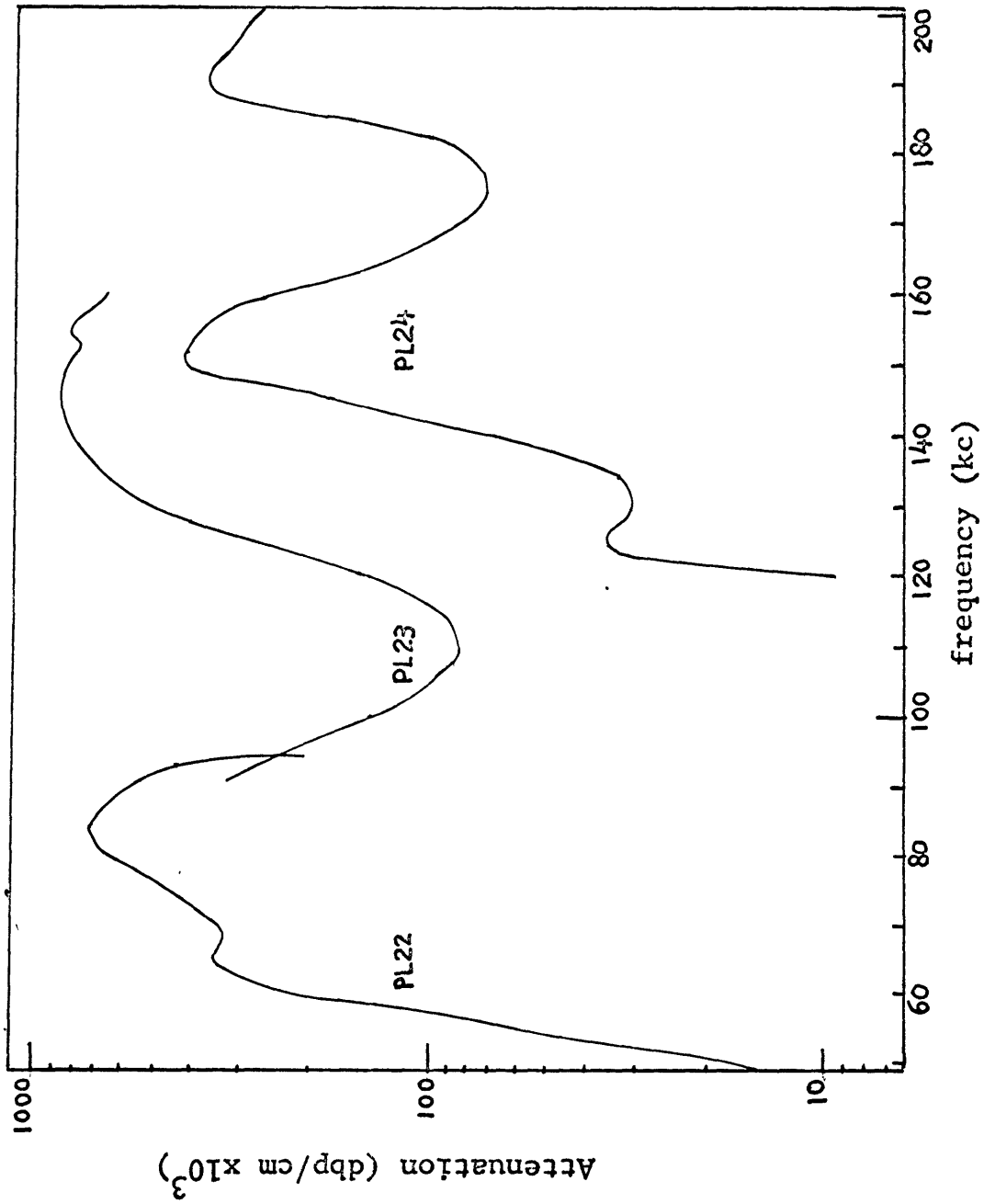

FIGURE 19

FOURIER TRANSFORM OF SMOOTHING OPERATOR

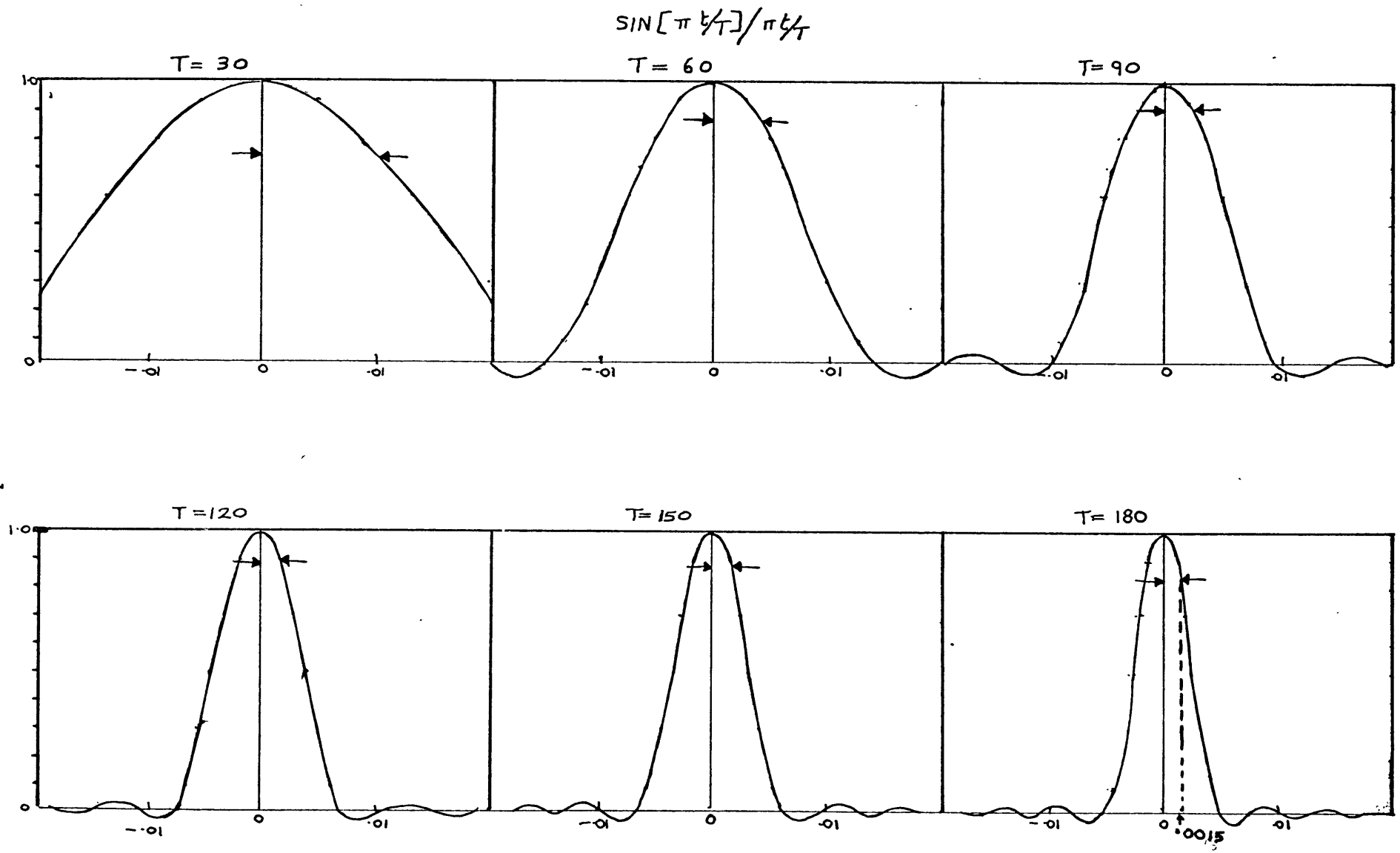

FIGURE 20

FOURIER TRANSFORM OF
FINITE UNIFORM SAMPLING OPERATOR